Table 2: Factors associated with response to peginterferon alfa-2b and ribavirin therapy.

	SVR	(Range or %)	Non-SVR	(Range or %)	*P* value
Total	74		26		
Age (y.o.)	57	(24–72)	57	(31–78)	NS
Sex (%)					
Male	33	(45)	13	(50)	
Female	41	(55)	13	(50)	NS
BMI (kg/m^2)	23.1	(15.4–30.9)	21.0	(18.4–26.0)	NS
WBC (/μL)	5100	(2100–9730)	5145	(3000–8300)	NS
Hemoglobin (g/dL)	14.1	(10–16)	14.0	(10–16)	NS
Platelet (10^4/μL)	21.7	(6.9–26.5)	11.5	(7.3–21.1)	NS
AST (IU/L)	39	(17–377)	44	(17–140)	NS
ALT (IU/L)	51	(11–751)	53	(14–169)	NS
TC (mg/dL)	183	(106–269)	163	(127–248)	NS
<177 mg/dL (%)	31	(42)	19	(73)	
≥177 mg/dL (%)	43	(58)	7	(27)	0.005
TG (mg/dL)	98	(56–262)	83	(74–176)	NS
<88 mg/dL (%)	33	(44)	17	(67)	
≥88 mg/dL (%)	41	(56)	9	(33)	NS
LDL-C (mg/dL)	109	(30–167)	88	(64–117)	0.015
<98 mg/dL (%)	30	(40)	20	(77)	
≥98 mg/dL (%)	44	(60)	6	(23)	0.020
HCV RNA (KIU/mL)	1000	(20–40900)	1850	(37–24200)	NS
Distribution of stage of fibrosis (%)					
1	31	(42)	12	(46)	
2	14	(19)	3	(12)	
3	6	(8)	5	(19)	
4	3	(4)	1	(4)	
Unknown	20	(27)	5	(19)	NS
Distribution of grade of inflammation (%)					
1	27	(36)	12	(46)	
2	25	(34)	9	(35)	
3	2	(3)	0	(0)	
Unknown	20	(27)	5	(19)	NS

Data are median (range) or frequency (%).

type 2 diabetes who is at low risk [21]. Furthermore, Miller et al. reported that American type 2 diabetic patients had an average cholesterol level of 179 mg/dL [22].

The reason for SVR improvement in patients with elevated serum cholesterol levels is unknown. In patients with chronic hepatitis B and hepatitis C, serum lipid levels have been reported to be correlated with specific cytokines that may have antiviral activity, including tumor necrosis factor-alpha and interleukin-6 [23]. This hyperlipidemia-induced increase in cytokine levels may have a favorable and potentially additive effect on antiviral treatment in patients with chronic hepatitis C. Another proposed mechanism may be related to a possible regulatory effect of cholesterol in HCV binding to cell surface receptors, which in turn may be relevant to viral clearance [24]. The LDL receptor, a membrane glycoprotein, has been shown to be involved in HCV entry into hepatocytes, and data suggest that HCV RNA levels correlate with LDL receptor expression [25, 26]. Elevated serum concentrations of LDL may decrease the number of LDL receptors located on hepatocytes.

Recent studies have shown that single nucleotide polymorphisms located in the gene region encoding interleukin 28b (IL28B) are strongly associated with the response to PEG-IFN and ribavirin therapy [17, 27, 28]. Total cholesterol, LDL cholesterol, and ApoB concentrations are significantly higher in chronic hepatitis C patients carrying a second IL28B major allele (CC in rs 12979860) compared with those possessing minor alleles (CT or TT) [29]. Therefore, the association between serum LDL cholesterol concentration and SVR may be reflected by the underlying link

Table 3: Univariate and multivariate analysis of the factors associated with SVR to peginterferon alfa-2b and ribavirin therapy.

		Univariate analysis		Multivariate analysis	
		P	RR (95% CI)	*P*	RR (95% CI)
Age	<57 years	0.646	1.24 (0.50–3.09)		
Sex	Female	0.634	0.80 (0.33–1.97)		
BMI	≥23 kg/m^2	0.221	1.86 (0.69–5.02)		
Underlying liver disease					
	CH	0.872	1.15 (0.21–6.32)		
WBC	≥5100 /μL	0.827	0.75 (0.37–2.22)		
Hb	≥14.0 g/dL	0.317	0.62 (0.25–1.58)		
Plt	≥20 × 10^4/μL	0.112	2.10 (0.84–5.24)		
AST	<40 IU/L	0.429	1.44 (0.58–3.55)		
ALT	<52 IU/L	0.649	1.23 (0.50–3.02)		
γ-GTP	<35 IU/L	0.525	0.75 (0.30–1.83)		
TC	≥177 mg/dL	0.008	3.77 (1.41–10.05)	0.015	18.59 (1.78–193.65)
TG	≥88 mg/dL	0.101	2.60 (0.83–8.13)		
LDL-C	≥98 mg/dL	0.028	4.91 (1.19–20.23)	0.800	1.25 (0.22–7.01)
Stage	F 3-4	0.419	0.60 (0.17–2.07)		
Grade	A 2-3	0.809	1.13 (0.41–3.18)		
HCV RNA					
	<1000 KIU/mL	0.310	1.65 (0.63–4.31)		

Relative risk (RR); 95% confidence interval (95% CI).

Table 4: Comparison between HCV patients with high and low serum TC.

TC	<177 mg/dL	(Range or %)	≥177 mg/dL	(Range or %)	*P* value
Total	50		50		
Age (y.o.)	57	(24–78)	57	(36–69)	NS
Sex (%)					
Male	34	(68)	20	(40)	
Female	16	(32)	30	(60)	0.005
BMI (kg/m^2)	21.5	(18.4–26.8)	23.5	(15.4–30.6)	0.027
WBC (/μL)	5100	(2100–9730)	5100	(3000–8300)	NS
Hemoglobin (g/dL)	14.2	(10–16)	13.9	(10–16)	NS
Platelet (10^4/μL)	17.6	(7.3–26.5)	21.7	(6.9–26.1)	NS
AST (IU/L)	48	(17–377)	33	(18–199)	0.033
ALT (IU/L)	67	(16–751)	40	(11–283)	NS
TG (mg/dL)	83	(46–203)	111	(43–262)	NS
<88 mg/dL (%)	32	(63)	19	(38)	
≥88 mg/dL (%)	18	(37)	31	(62)	0.045
LDL-C (mg/dL)	84	(43–118)	121	(30–167)	<0.001
<98 mg/dL (%)	40	(79)	9	(19)	
≥98 mg/dL (%)	10	(21)	41	(81)	<0.001
HCV RNA (KIU/mL)	1000	(20–24200)	2670	(20–40900)	0.029
Distribution of stage of fibrosis (%)					
1	18	(36)	25	(50)	
2	7	(14)	10	(20)	
3	8	(16)	3	(6)	
4	2	(4)	2	(4)	
Unknown	15	(30)	10	(20)	NS
Distribution of grade of inflammation (%)					
1	20	(40)	19	(38)	
2	14	(28)	20	(40)	
3	1	(2)	1	(2)	
Unknown	15	(30)	10	(20)	NS

Data are median (range) or frequency (%).

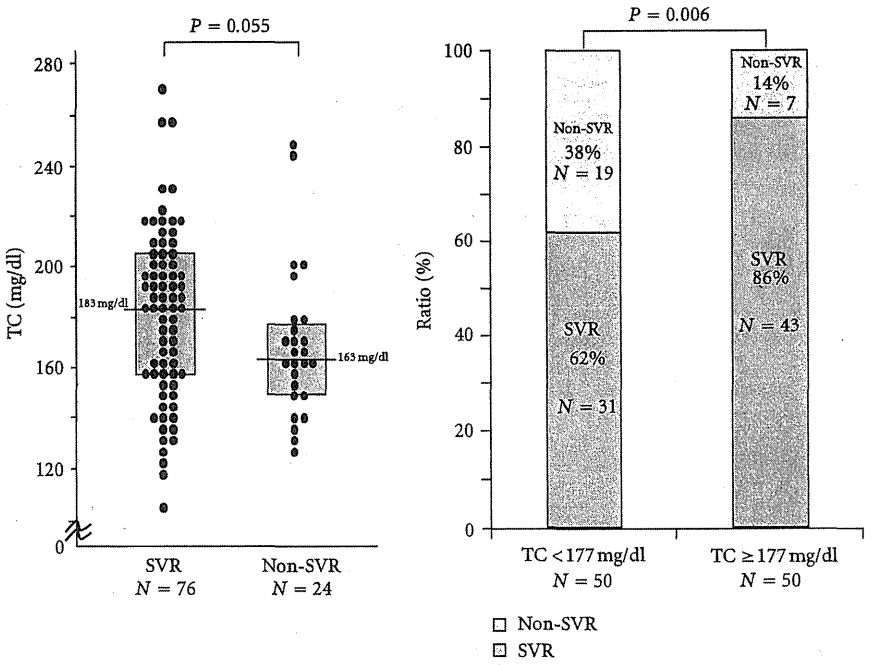

FIGURE 1: Comparison between SVR rate in patients with high serum TC levels (≥177 mg/dL) and patients with low serum TC levels (<177 mg/dL) in HCV genotype 2 patients.

between IL28B genotypes and LDL cholesterol concentrations. As discussed above, we cannot exclude the possibility that high cholesterol levels in patients with HCV only reflect the presence of the IL28B major allele. It may simply reflect the wild-type sequence at core amino acid 70 because substitution in the core protein correlated significantly with a low concentration of LDL cholesterol [30, 31]. However, we could not identify IL28-B and core amino acid 70 as predictive for our patients with HCV genotype 2 because our sample population was limited.

Petta and Craxì reported that age, sex, stage of fibrosis, and baseline viral load were important predictive factors SVR in patient with HCV genotype 2 [32]. However, our study was not significantly differente in these factors for SVR. Furthermore, there was no significant difference in the serum TC between SVR and non-SVR by the Mann-Whitney *U* test. The reason may be explained as follows: severe stage of fibrosis (F3-4) was recruited only 15%, and 25% was stage unknown in this study. HCV RNA in high TC group was significant higher than low TC group. Finally, this was the limitation small sample size and retrospective study. The discrepancies of the observation from different reports need further investigation.

In conclusion, our data suggest that baseline serum total cholesterol levels should be considered when assessing the likelihood of sustained treatment response following PEG-IFN and ribavirin therapy in patients with chronic HCV genotype 2 infection. However, this finding requires further analysis.

Conflict of Interests

The authors declare that they have no conflict of interests and financial support.

References

[1] J. M. Barrera, M. Bruguera, M. G. Ercilla et al., "Persistent hepatitis C viremia after acute self-limiting posttransfusion hepatitis C," *Hepatology*, vol. 21, no. 3, pp. 639–644, 1995.

[2] F. Penin, J. Dubuisson, F. A. Rey, D. Moradpour, and J. M. Pawlotsky, "Structural biology of hepatitis C virus," *Hepatology*, vol. 39, no. 1, pp. 5–19, 2004.

[3] S. J. Hadziyannis, H. Sette, T. R. Morgan et al., "Peginterferon-alpha2a and ribavirin combination therapy in chronic hepatitis C: a randomized study of treatment duration and ribavirin dose," *Annals of Internal Medicine*, vol. 140, no. 5, pp. 346–355, 2004.

[4] M. P. Manns, J. G. McHutchison, S. C. Gordon et al., "Peginterferon alfa-2b plus ribavirin compared with interferonalfa-2b plus ribavirin for initial treatment of chronic hepatitis C: a randomised trial," *The Lancet*, vol. 358, no. 9286, pp. 958–965, 2001.

[5] J. Ye, "Reliance of host cholesterol metabolic pathways for the life cycle of hepatitis C virus," *PLoS Pathogens*, vol. 3, no. 8, p. e108, 2007.

[6] K. Ogawa, T. Hishiki, Y. Shimizu et al., "Hepatitis C virus utilizes lipid droplet for production of infectious virus," *Proceedings of the Japan Academy B*, vol. 85, no. 7, pp. 217–228, 2009.

[7] F. Negro and A. J. Sanyal, "Hepatitis C virus, steatosis and lipid abnormalities: clinical and pathogenic data," *Liver International*, vol. 29, supplement 2, pp. 26–37, 2009.

[8] K. Gopal, T. C. Johnson, S. Gopal et al., "Correlation between beta-lipoprotein levels and outcome of hepatitis C treatment," *Hepatology*, vol. 44, no. 2, pp. 335–340, 2006.

[9] M. Economou, H. Milionis, S. Filis et al., "Baseline cholesterol is associated with the response to antiviral therapy in chronic hepatitis C," *Journal of Gastroenterology and Hepatology*, vol. 23, no. 4, pp. 586–591, 2008.

[10] D. Ramcharran, A. S. Wahed, H. S. Conjeevaram et al., "Associations between serum lipids and hepatitis C antiviral treatment efficacy," *Hepatology*, vol. 52, no. 3, pp. 854–863, 2010.

[11] P. Ferenci, M. W. Fried, M. L. Shiffman et al., "Predicting sustained virological responses in chronic hepatitis C patients treated with peginterferon alfa-2a (40 KD)/ribavirin," *Journal of Hepatology*, vol. 43, no. 3, pp. 425–433, 2005.

[12] Y. Inoue, N. Hiramatsu, T. Oze et al., "Factors affecting efficacy in patients with genotype 2 chronic hepatitis C treated by pegylated interferon alpha-2b and ribavirin: reducing drug doses has no impact on rapid and sustained virological responses," *Journal of Viral Hepatitis*, vol. 17, no. 5, pp. 336–344, 2010.

[13] V. J. Desmet, M. Gerber, J. H. Hoofnagle, M. Manns, and P. J. Scheuer, "Classification of chronic hepatitis: diagnosis, grading and staging," *Hepatology*, vol. 19, no. 6, pp. 1513–1520, 1994.

[14] M. Romero-Gómez, M. Del Mar Viloria, R. J. Andrade et al., "Insulin resistance impairs sustained response rate to peginterferon plus ribavirin in chronic hepatitis C patients," *Gastroenterology*, vol. 128, no. 3, pp. 636–641, 2005.

[15] P. Marotta, D. Hueppe, E. Zehnter, P. Kwo, and I. Jacobson, "Efficacy of chronic hepatitis C therapy in community-based trials," *Clinical Gastroenterology and Hepatology*, vol. 7, no. 10, pp. 1028–1036, 2009.

[16] S. Maekawa and N. Enomoto, "Viral factors influencing the response to the combination therapy of peginterferon plus ribavirin in chronic hepatitis C," *Journal of Gastroenterology*, vol. 44, no. 10, pp. 1009–1015, 2009.

[17] D. L. Thomas, C. L. Thio, M. P. Martin et al., "Genetic variation in IL28B and spontaneous clearance of hepatitis C virus," *Nature*, vol. 461, no. 7265, pp. 798–801, 2009.

[18] G. Y. Minuk, S. Weinstein, and K. D. Kaita, "Serum cholesterol and low-density lipoprotein cholesterol levels as predictors of response to interferon therapy for chronic hepatitis C," *Annals of Internal Medicine*, vol. 132, no. 9, pp. 761–762, 2000.

[19] G. Testino and P. Borro, "Hepatitis C recurrence: influence of serum cholesterol levels and liver steatosis on antiviral therapy," *Hepatology*, vol. 53, no. 4, pp. 1409–1410, 2011.

[20] E. Villa, A. Karampatou, C. Camm et al., "Early menopause is associated with lack of response to antiviral therapy in women with chronic hepatitis C," *Gastroenterology*, vol. 140, no. 3, pp. 818–829, 2011.

[21] S. Haffner, "Rationale for new American Diabetes Association Guidelines: are national cholesterol education program goals adequate for the patient with diabetes mellitus?" *American Journal of Cardiology*, vol. 96, no. 4, pp. 33E–36E, 2005.

[22] C. D. Miller, L. S. Phillips, M. K. Tate et al., "Meeting American Diabetes Association guidelines in endocrinologist practice," *Diabetes Care*, vol. 23, no. 4, pp. 444–448, 2000.

[23] C. Fabris, E. Federico, G. Soardo, E. Falleti, and M. Pirisi, "Blood lipids of patients with chronic hepatitis: differences related to viral etiology," *Clinica Chimica Acta*, vol. 261, no. 2, pp. 159–165, 1997.

[24] M. Monazahian, I. Böhme, S. Bonk et al., "Low density lipoprotein receptor as a candidate receptor for hepatitis C virus," *Journal of Medical Virology*, vol. 57, no. 3, pp. 223–229, 1999.

[25] J. M. Petit, A. Minello, L. Duvillard et al., "Cell surface expression of LDL receptor in chronic hepatitis C: correlation with viral load," *American Journal of Physiology*, vol. 293, no. 1, pp. E416–E420, 2007.

[26] S. Molina, V. Castet, C. Fournier-Wirth et al., "The low-density lipoprotein receptor plays a role in the infection of primary human hepatocytes by hepatitis C virus," *Journal of Hepatology*, vol. 46, no. 3, pp. 411–419, 2007.

[27] D. Ge, J. Fellay, A. J. Thompson et al., "Genetic variation in IL28B predicts hepatitis C treatment-induced viral clearance," *Nature*, vol. 461, no. 7262, pp. 399–401, 2009.

[28] V. Suppiah, M. Moldovan, G. Ahlenstiel et al., "IL28B is associated with response to chronic hepatitis C interferon-α and ribavirin therapy," *Nature Genetics*, vol. 41, no. 10, pp. 1100–1104, 2009.

[29] J. H. Li, X. Q. Lao, H. L. Tillmann et al., "Interferon-lambda genotype and low serum low-density lipoprotein cholesterol levels in patients with chronic hepatitis C infection," *Hepatology*, vol. 51, no. 6, pp. 1904–1911, 2010.

[30] K. Chayama, C. N. Hayes, K. Yoshioka et al., "Accumulation of refractory factors for pegylated interferon plus ribavirin therapy in older female patients with chronic hepatitis C," *Hepatology Research*, vol. 40, no. 12, pp. 1155–1167, 2010.

[31] A. Honda and Y. Matsuzaki, "Cholesterol and chronic hepatitis C virus infection," *Hepatology Research*, vol. 41, no. 8, pp. 697–710, 2011.

[32] S. Petta and A. Craxì, "Optimal therapy in hepatitis C virus genotypes 2 and 3 patients," *Liver International*, vol. 31, supplement 1, pp. 36–44, 2011.

J Gastroenterol
DOI 10.1007/s00535-012-0656-2

ORIGINAL ARTICLE—LIVER, PANCREAS, AND BILIARY TRACT

Accumulation of platelets in the liver may be an important contributory factor to thrombocytopenia and liver fibrosis in chronic hepatitis C

Reiichiro Kondo · Hirohisa Yano · Osamu Nakashima · Ken Tanikawa · Yoriko Nomura · Masayoshi Kage

Received: 3 April 2012 / Accepted: 25 July 2012

Abstract
Background Thrombocytopenia is a marked feature of chronic liver disease and cirrhosis. We tried to clarify whether an accumulation of platelets in the liver contributes to thrombocytopenia and liver fibrosis in chronic liver disease.
Methods Thirty-eight patients who underwent hepatectomy for hepatocellular carcinoma (HCC) with hepatitis C virus infection were included. The locations of platelets and Kupffer cells and the expression of platelet-derived growth factor (PDGF) receptor-β and smooth muscle actin (SMA) were identified by immunohistochemistry. Perisinusoidal mesenchymal cells that express PDGF receptor-β and SMA were interpreted as transformed hepatic stellate cells (HSCs).
Results Patients with cirrhosis had a more extensive platelet area in the liver compared to controls (5601 ± 5611 vs. 564 ± 361 μm^2, $p = 0.02$), although the blood platelet count significantly decreased along with the progression of liver fibrosis. In cirrhotic liver, most platelets were present in the sinusoidal space of the periportal area with inflammation, where HSCs expressing PDGF receptor-β were frequently observed. In addition, the platelet and Kupffer cell areas were significantly smaller in cancerous tissue than those in noncancerous tissues (platelet area: 492 ± 823 vs. 3643 ± 4055 μm^2, $p = 0.001$; Kupffer cell area: 450 ± 841 vs. 3012 ± 3051 μm^2, $p = 0.001$).
Conclusions The accumulation of platelets in the liver with chronic hepatitis may be involved in thrombocytopenia and liver fibrosis through the activation of HSCs. In addition, our findings also indicate that both platelets and Kupffer cells decrease in HCC tissues.

Keywords Platelet · PDGFR-β · Hepatic stellate cells · Sinusoidal endothelial cells

Introduction

Blood platelets, besides hemostatic properties, have the features of inflammatory cells. Blood platelets, while activated in inflammatory processes, release active compounds: platelet-derived growth factors (PDGF), vascular endothelial growth factor (VEGF), transforming growth factor (TGF)-β, and so forth [1]. Platelets transport these active compounds to the target cells [2, 3]. There are many reports presenting multipotential properties of blood platelets, such as angiogenesis [4–6], wound healing [7, 8], liver regeneration [9], and metastasis in cancer [6, 10, 11]. In acute viral hepatitis, platelets mediate cytotoxic T lymphocyte-induced liver damage [12]. After virus infection, platelets were recruited to the liver, delaying virus elimination and increasing immunopathological liver cell damage [13].

In chronic hepatitis, the blood platelet level gradually decreases, which is reflected in liver fibrosis. Blood

R. Kondo (✉) · H. Yano · K. Tanikawa · Y. Nomura
Department of Pathology, Kurume University School of Medicine, 67 Asahi-machi, Kurume, Fukuoka 830-0011, Japan
e-mail: kondou_reiichirou@kurume-u.ac.jp

R. Kondo · Y. Nomura · M. Kage
Department of Diagnostic Pathology, Kurume University Hospital, 67 Asahi-machi, Kurume, Fukuoka, Japan

O. Nakashima
Department of Clinical Laboratory Medicine, Kurume University Hospital, 67 Asahi-machi, Kurume, Fukuoka, Japan

M. Kage
Research Center for Innovative Cancer Therapy, Kurume University School of Medicine, 67 Asahi-machi, Kurume, Fukuoka, Japan

Published online: 22 August 2012

platelets and chronic liver disease are also closely related. Thrombocytopenia is a marked feature of chronic liver disease and cirrhosis. Cirrhosis is a major cause of morbidity and mortality in many countries, and results in liver failure, portal hypertension, and increased risk of carcinogenesis [14]. The main causes of liver fibrosis include chronic hepatitis C virus infection, alcohol abuse, and nonalcoholic steatohepatitis [15]. The role of platelets in the pathogenesis of liver damage and the exact mechanisms leading to thrombocytopenia in cirrhosis are not yet clear [16]. The thrombocytopenia that occurs in cirrhosis is most likely due to various processes, including increased splenic platelet breakdown [17–19], splenic pooling [20, 21], and the inability of the bone marrow to increase platelet production adequately [22]. According to previous reports assessing the feasibility of platelet scintigraphy, an accumulation of platelets in the liver was observed in patients presenting with thrombocytopenia [17–20, 23–25]. Based on these findings, thrombocytopenia with chronic hepatitis and cirrhosis may be caused by hypersplenism, as well as by the capture of platelets by the liver. However, the platelet kinetics of patients with chronic liver disease are not well characterized. Therefore, the aim of the study described in the present paper was to clarify the histopathological findings of platelets in human liver tissue and to elucidate the role of platelets in the pathogenesis of chronic liver disease.

Methods

Tissues

We studied 38 patients who underwent hepatectomy for hepatocellular carcinoma (HCC) with hepatitis C viral infection at the Kurume University Hospital; their clinical backgrounds are shown in Table 1. These cases did not receive preoperative anticancer therapies. Both cancerous tissues and adjacent noncancerous liver tissues were obtained by surgical operation.

Five specimens of liver tissues obtained from patients who underwent hepatectomy for hepatic cavernous hemangioma without chronic hepatitis were used as controls.

The study was performed with informed consent obtained from patients for the use of their liver tissues in the investigation, and was approved by the ethical committee at Kurume University (approved ID number: 11200).

Histopathology

Each tissue was fixed with 10 % formalin, embedded in paraffin, cut into 5 μm sections, and then used for histological and immunohistological analyses. The specimens were stained with hematoxylin and eosin and examined under a light microscope. The histological liver damage of these specimens was evaluated for fibrosis and inflammation according to the classification proposed by the International Association for the Study of the Liver [26, 27]. The severity of fibrosis (stage of disease) was classified as none (stage 0), mild (portal fibrosis; stage 1), moderate (periportal fibrosis; stage 2), severe (bridging fibrosis with lobar distortion; stage 3), and cirrhosis (stage 4), and the inflammatory activity (grade of disease activity) was classified as none (grade 0), minimal (grade 1), mild (grade 2), moderate (grade 3), or severe (grade 4). The pathological features of HCC were evaluated according to the World Health Organization classification [28].

Histopathological diagnosis and classification were performed by four pathologists (R.K., H.Y., O.N., and M.K.).

Table 1 Clinical features of the patients studied in this work

Stage	1	2	3	4
No. of subjects	10	10	8	10
Sex (male/female)	8/2	9/1	6/2	5/5
Age (years)[a]	74 ± 5.0	71 ± 6.9	69 ± 9.9	74 ± 4.2
Grade (1/2)	7/3	3/7	1/7	1/9
Platelet count ($\times 10^4$)[a]	15.8 ± 3.4	13.5 ± 2.5	11.8 ± 5.1	10.6 ± 2.5
HCC (well/moderate/poor)	0/10/0	1/8/1	1/7/0	0/10/0

The severity of fibrosis was classified as none: stage 0, portal fibrosis: stage 1, periportal fibrosis: stage 2, bridging fibrosis with lobar distortion: stage 3, and cirrhosis: stage 4. The inflammatory activity was classified as none: grade 0, minimal: grade 1, mild: grade 2, moderate: grade 3, or severe: grade 4

HCC hepatocellular carcinoma, *well* well differentiated HCC, *moderate* moderately differentiated HCC, *poor* poorly differentiated HCC

[a] Mean ± SD

Immunohistochemical analysis

The avidin–biotin peroxidase complex method was used for immunohistochemistry. We used monoclonal antibodies against CD41 (1:500, Beckman Coulter, Brea, CA, USA), CD68 (1:200, DAKO, Glostrup, Denmark), PDGF receptor-β (1:200, Santa Cruz Biotechnology, Santa Cruz, CA, USA) and smooth muscle actin (1:200, DAKO). CD41 (glycoprotein IIb/IIa complex) is a specific marker for platelets, so a CD41-positive reaction was taken to indicate the presence of platelets. CD68, an anti-human macrophage antibody, is expressed not only in residential macrophages such as Kupffer cells, but also in migrating macrophages. Among

the CD68-positive cells, those in the sinusoidal space or blood space of cancerous tissues with spindle or stellate-shaped cytoplasm, and those partly adhering to the sinusoidal endothelial cells, were evaluated as Kupffer cells. Perisinusoidal mesenchymal cells express PDGF receptor-β as transformed hepatic stellate cells (HSCs) [29–31]. These cells were evaluated as activated HSCs.

Measurement of cells

The area of platelets and Kupffer cells in each specimen was measured using the WinROOF software package (version 6.1, Mitani Corporation, Fukui, Japan). In noncancerous liver tissues, the areas were measured in five randomly selected periportal regions. In cancerous tissues, five visual fields were randomly selected.

Transmission electron microscopy

The liver was cut into small pieces (approximately 1 mm^3), the specimens were fixed in 2.5 % glutaraldehyde in 0.1 M phosphate buffer, pH 7.4, and they were then post-fixed in 1 % O_8O_4 in 0.1 M phosphate buffer. Next, the specimens were dehydrated through a graded series of ethanol, passed through propylene oxide, and embedded in Epok 812. Ultrathin sections mounted on copper grids were stained with uranyl acetate and lead citrate and observed in a Hitachi (Tokyo, Japan) H-7650 transmission electron microscope.

Statistical analysis

The arithmetic means and standard deviations of our data were calculated using the JMP software package (release 9.0, SAS Institute, Cary, NC, USA). All data are expressed as mean $\pm$ SD, and p values of less than 5 % were considered to indicate significance.

Results

Histological findings

Noncancerous liver tissues of all patients with hepatitis C virus infection showed various degrees of fibrosis and chronic inflammation. The severity of fibrosis was mild (stage 1) in ten patients, moderate (stage 2) in ten patients, and severe (stage 3) in eight patients, while ten patients had cirrhosis (stage 4). The inflammatory activity was minimal (grade 1) in 12 patients and mild (grade 2) in 26 patients. In control tissues, there were a few lymphocytes, but only in the portal area, and neither necroinflammatory reactions nor fibrosis were noted (grade 0, stage 0).

Among the cancerous tissues in 38 cases, 35 cases were moderately differentiated HCCs, two cases were well-differentiated HCCs, and one case was poorly differentiated HCC. In terms of the diameters of the HCCs, there were two cases with an HCC diameter of $\leq$1.0 cm, 11 cases with a diameter of 1.1–2.0 cm, 14 cases with 2.1–3.0 cm, and 11 cases with $\geq$3.0 cm. Comparing the histological differentiation of cancerous tissues, the mean tumor size was 2.6 $\pm$ 0.6 cm in the well-differentiated HCCs, 3.0 $\pm$ 1.8 cm in the moderately differentiated HCCs, and 6.3 cm in the poorly differentiated HCCs. Among the 37 nodular-type HCCs, 24 specimens had clear fibrous capsules at the tumor and nontumor boundary, while 13 cases had no fibrous capsules.

Platelets in noncancerous liver tissues

In all noncancerous liver tissues, including patients with chronic hepatitis or cirrhosis and in the controls, there were platelets but no megakaryocytes in the sinusoidal space. Patients with cirrhosis had a more extensive platelet area in the noncancerous liver tissue than in controls (5601 $\pm$ 5611 vs. 564 $\pm$ 361 μm^2, $p = 0.02$, $p < 0.05$, Fig. 1a). In patients with chronic hepatitis or cirrhosis, the platelet area in noncancerous liver tissues increased along with an increase in histological liver damage ($p = 0.02$, $p < 0.05$), although the blood platelet count significantly decreased (Fig. 1b). In noncancerous liver tissues with chronic hepatitis or cirrhosis, platelets were present predominantly in the sinusoidal space of the periportal area with inflammation. In high-stage cases, platelets were observed along the destroyed limiting plate of the expanded fibrous portal area with inflammation, and in the sinusoidal space of the periportal area (Fig. 2).

Relationship among platelets, HSCs, and Kupffer cells in non-cancerous liver tissues

Immunohistochemical studies of noncancerous liver tissues with cirrhosis revealed that most platelets were present in the periportal area with inflammation, where HSCs expressing PDGF receptor-β were frequently observed (Fig. 3a, b). Most smooth muscle actin stained cells were identical to those expressing PDGF receptor-β (Fig. 3c). In noncancerous liver tissues of controls and cases at the lower stage of chronic hepatitis, only a few HSCs expressing PDGF receptor-β were seen.

In noncancerous liver tissues, including patients with chronic hepatitis or cirrhosis and in controls, CD68-positive Kupffer cells were seen in the sinusoidal spaces of both periportal and lobular areas diffusely.

Platelets and Kupffer cells in cancerous tissues

In all cancerous tissues, a few platelets and Kupffer cells were present in the blood spaces of cancerous tissues.

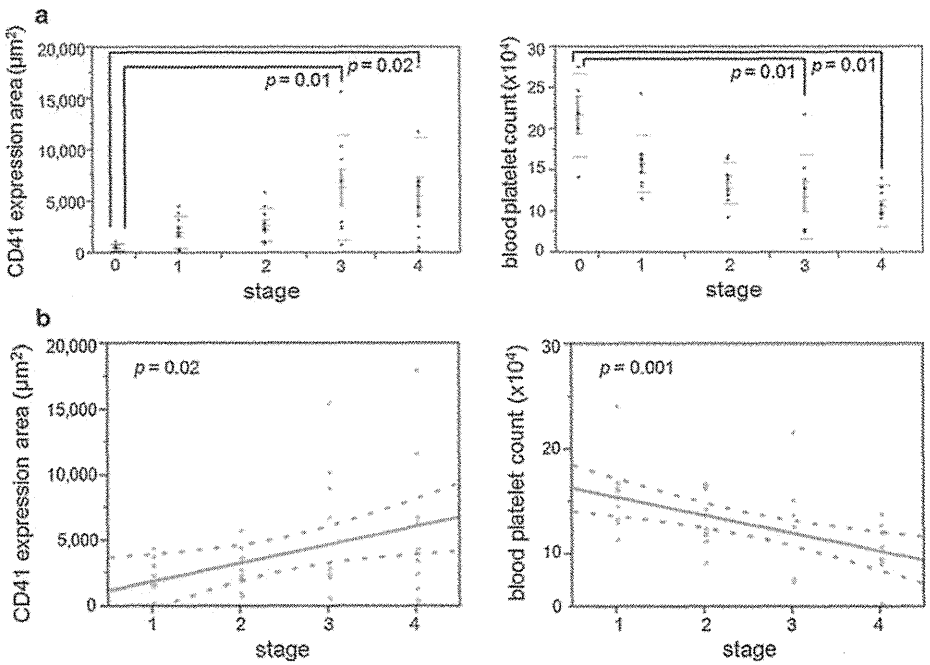

Fig. 1 Relationship between histological liver damage and either the CD41 expression area in the noncancerous liver tissues or the blood platelet count. **a** The noncancerous liver tissues with cirrhosis had a larger CD41 expression area than seen in the controls ($p = 0.02$, $p < 0.05$), although the blood platelet count was small. **b** In the noncancerous liver tissues with chronic hepatitis and cirrhosis, the CD41 expression area increased with increasing histological liver damage ($p = 0.02$, $p < 0.05$), although the blood platelet count decreased ($p = 0.001$, $p < 0.05$)

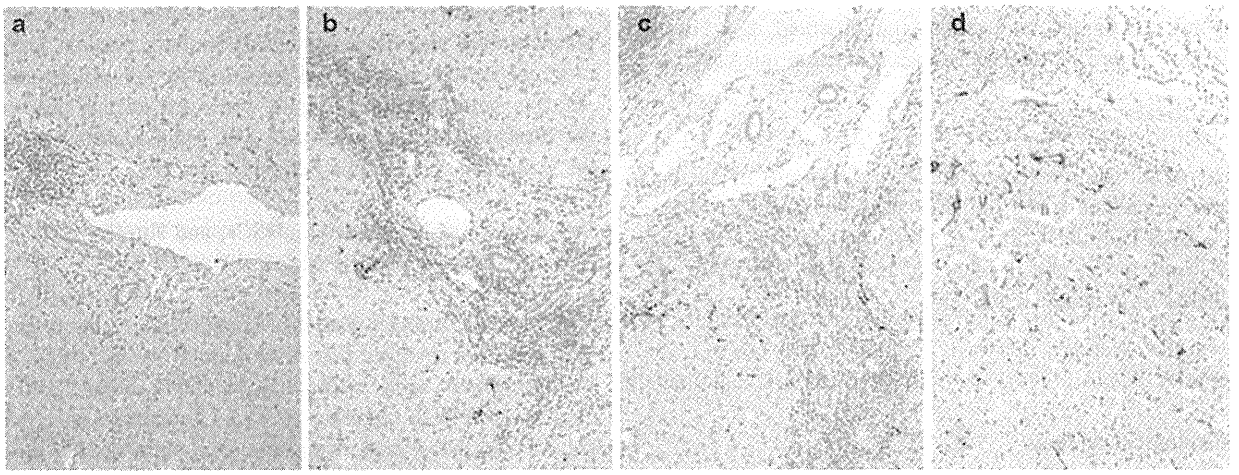

Fig. 2 Typical immunostaining for CD41 in a periportal area of noncancerous liver tissues with chronic hepatitis or cirrhosis. In noncancerous liver tissues with chronic hepatitis or cirrhosis, CD41-positive reactions are present predominantly in the sinusoidal space of the periportal area with inflammation. In high-stage cases, strong CD41 positive reactions are observed along the destroyed limiting plate of the expanded fibrous portal area with inflammation, and in the sinusoidal space of the periportal area. Labeled streptavidin biotin with CD41 antibody: **a** grade 1, stage 1; **b** grade 2, stage 2; **c** grade 2, stage 3; **d** grade 2, stage 4

When the platelet and Kupffer cell areas in the cancerous and non-cancerous tissues were compared, the platelet and Kupffer cell areas were significantly smaller in cancerous tissue than in noncancerous tissue (Fig. 4a, platelet area: 492 ± 823 vs. 3643 ± 4055 μm^2, $p = 0.001$, $p < 0.05$; Fig. 4b, Kupffer cell area: 450 ± 841 vs. 3012 ± 3051 μm^2, $p = 0.001$, $p < 0.05$). Regardless of the liver damage in noncancerous tissue, both the platelet and Kupffer cell areas in cancerous tissue were smaller than those in noncancerous tissue. The platelet and Kupffer cell areas in cancerous tissue tended to decrease with decreasing histological differentiation of HCC (Table 2). We also measured with regard to the

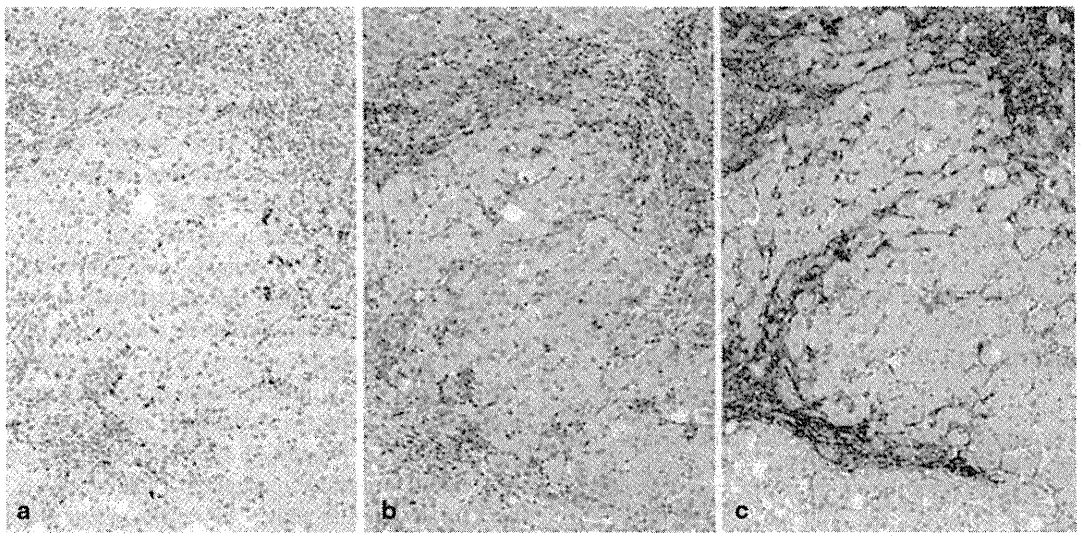

Fig. 3 Typical immunostaining for CD41, PDGF receptor-β, and smooth muscle actin in the periportal area of noncancerous liver tissues with cirrhosis. **a** Platelets are present in the periportal area with inflammation. Labeled streptavidin biotin with CD41 antibody. **b** Serial section shown in **a** stained for PDGF receptor-β antibody. Portal mesenchymal and perisinusoidal cells are stained for PDGF receptor-β. These are dense in the periportal area, where platelets are frequently observed in **a**. Labeled streptavidin biotin with PDGF receptor-β antibody. **c** Serial section shown in **b** stained with smooth muscle actin. Most of the stained cells are identical to those stained for PDGF receptor-β in **b**. Labeled streptavidin biotin with smooth muscle actin antibody

Kupffer cell count. The results evaluated by Kupffer cell count correlate with those evaluated by Kupffer cell areas. The Kupffer cell count was significantly smaller in cancerous tissue than in noncancerous tissue (data was not shown).

Electron microscopic findings

In the sinusoidal space of noncancerous tissues with cirrhosis, there were platelets with dense granules and α-granules. They were partly attached to the sinusoidal endothelial cells (Fig. 5a). Some of the platelets had several empty granules, which are indicative of degranulation (Fig. 5b). Platelets were rarely found in the space of Disse. Around platelets that adhered to the sinusoidal endothelial cells, HSCs that were more spindle-shaped and had a few fat droplets were observed (Fig. 5c). Platelets were not in direct contact with HSCs and Kupffer cells.

Discussion

Blood platelets, by connecting hemostasis and inflammatory processes, participate in the pathogenesis of chronic liver disease. In this study, we demonstrated the pathological findings for the accumulation of platelets in the liver in cases with chronic hepatitis C.

Hill-Zobel et al. [32] studied platelet dynamics in healthy humans using ^{111}In-labeled platelets. They reported

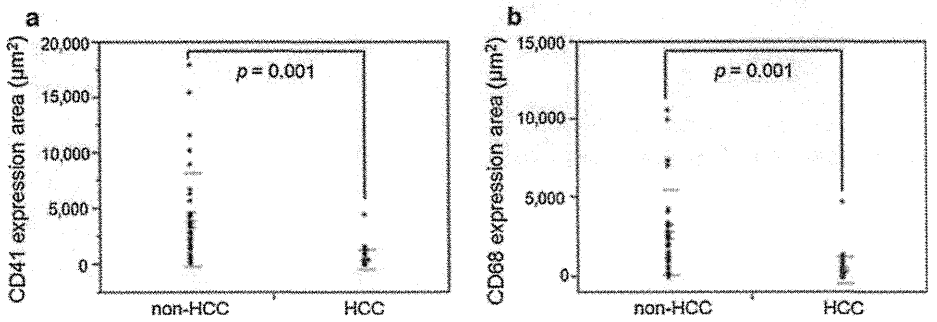

Fig. 4 CD41 (**a**) and CD68 (**b**) expression areas in different tissue types (HCC vs. non-HCC). Both the platelet and Kupffer cell areas are significantly smaller in HCC tissue than those in nonHCC tissue (platelet area: 492 ± 823 vs. 3643 ± 4055 μm^2, $p = 0.001$, $p < 0.05$; Kupffer cell area: 450 ± 841 vs. 3012 ± 3051 μm^2, $p = 0.001$, $p < 0.05$)

that the uptake in the liver was 12.6 % at 30 min and 24 % at ten days, and that in the spleen was 42.7 % at 30 min and 37 % at ten days in healthy humans [32]. The accumulation of platelets in the normal control liver tissue was confirmed in this study. However, the platelet dynamics of patients with chronic hepatitis or cirrhosis are not yet clear. In the current study, we found that the accumulation of platelets in noncancerous liver tissues of patients with chronic hepatitis or cirrhosis increased with increasing histological liver damage. In patients with chronic hepatitis or cirrhosis, the blood platelet level gradually decreased, and was reflected in the liver damage. As there are no megakaryocytes in liver tissues, we can distinguish between platelets that have accumulated in the sinusoidal space and are derived from bone marrow from those derived from extramedullary hematopoiesis. The extramedullary hematopoietic tissue should have hematinic cells, such as megakaryocytes, and immature cells. The accumulation of platelets in the cirrhotic liver with thrombocytopenia has been shown using platelet scintigraphy [17, 23–25]. In patients with thrombocytopenia, Kinuya et al. [24] reported that the spleen/liver uptake ratio for ^{111}In- or ^{99}Tc-labeled platelets was apparently lower in patients for whom splenectomy is ineffective than in those for whom it was effective. Sata et al. [25] reported that platelets were captured in the liver during interferon therapy for chronic hepatitis B, and that this phenomenon is one cause of the decrease in peripheral blood platelets during interferon therapy. The results of our present study are not necessarily contrary to the established theory of thrombocytopenia with chronic hepatitis. It has been reported that the mechanisms leading to thrombocytopenia in cirrhosis most likely involve multifactorial processes [17–22]. We consider that the accumulation of platelets in the liver with chronic hepatitis and cirrhosis may be one of the important contributory factors to thrombocytopenia.

Table 2 Relationship between histological differentiation and platelet area or Kupffer cell area in HCCs

Histological differentiation	Platelet area (μm^2)	Kupffer cell area (μm^2)
Well ($n = 2$)[a]	1532 ± 26	2674 ± 3094
Moderate ($n = 35$)[a]	440 ± 82	305 ± 405
Poor ($n = 1$)	225	108

well well differentiated HCC, *moderate* moderately differentiated HCC, *poor* poorly differentiated HCC

[a] Mean ± SD

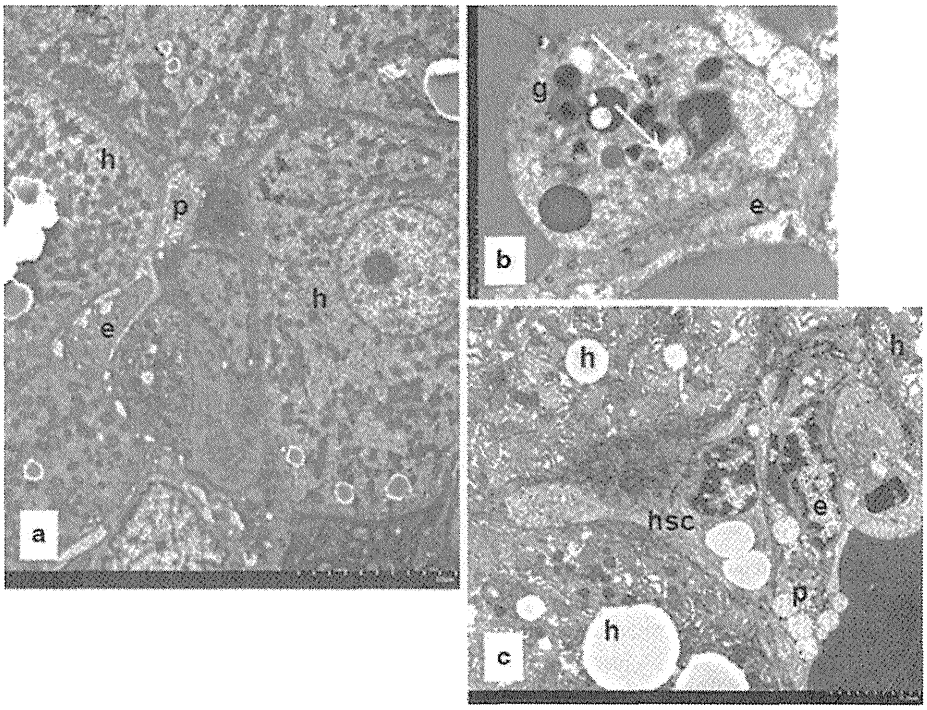

Fig. 5 Electron micrographs of a cirrhotic liver. **a** Platelets (*p*) in the sinusoidal space adhere to endothelial cells (*e*). **b** A platelet that has adhered to a sinusoidal endothelial cell contains both α-granules (*g*) and empty ones (*arrows*). **c** Around platelets that have adhered to a sinusoidal endothelial cell, a hepatic stellate cell (*hsc*)—which is more spindle-shaped, and has a few fat droplets—can be observed. *h* hepatocytes; **a** ×5000, **b** ×25000; **c** ×7000

Histologically, platelets in noncancerous liver tissues of patients with chronic hepatitis or cirrhosis are seen predominantly in the sinusoidal space of the periportal area with inflammation. As viewed through an electron microscope, the platelets aggregate in the sinusoids and adhere to the sinusoidal endothelial cells. Platelets contain four types of distinguishable granules or vesicles: dense granules, lysosomes, peroxisomes, and α-granules. These granules contain various active compounds. Blood platelets, activated in inflammatory and immune processes, release different intraplatelet compounds [1]. Platelets transport these active compounds in their granules to the target cells [2, 3]. Platelets then adhere to endothelial cells or exposed subendothelial matrices. Following adhesion, they become activated and secrete granule content. The accumulation of platelets in the liver and the adhesion to the sinusoidal endothelial cells are important steps in direct platelet action for the liver. In blood vessels, the vessel wall, with its inner lining of endothelium, is crucial to the maintenance of a patent vasculature. The endothelium contains thromboregulators—nitric oxide, prostacyclin, and the ectonucleotidase CD39—which together provide a defence against platelet thrombus formation [33]. When the endothelium is disrupted, collagen and tissue factor become exposed to the flowing blood, thereby initiating the formation of thrombus. Endothelium is also an important target for tumor necrosis factor (TNF) and interleukin-1 (IL-1). The endothelium synthesizes and releases platelet activating factor (PAF) in response to TNF. This activity of TNF overlaps that of IL-1, which also induces PAF production in endothelium [34]. These vessel wall alterations result in a change in endothelium from antithrombotic to thrombotic. The disrupted endothelium is the first reaction in platelet adhesion to the vessel subendothelium under physiologic blood flow [33]. In the presence of TNF-α-induced sinusoidal alteration, platelets adhere to sinusoidal endothelial cells in the same way as to vessel walls [35]. Characteristic pathological features of chronic HCV infection are chronic inflammation and apoptosis of infected and bystander hepatocytes [36, 37]. In a model of hepatitis, Kupffer cells produced the majority of TNF-α [38]. Under lipopolysaccharide administration in mice, TNF or IL-1 induce platelets to accumulate in the liver sinusoidal space within a few minutes by a different mechanism of aggregation [39–41]. With the depletion of Kupffer cells, platelets do not accumulate in the liver after lipopolysaccharide administration [41]. Kupffer cells are involved in various mechanisms, such as phagocytosis, metabolism, cytokine generation, and antitumor effect. Platelets may accumulate in the sinusoidal space under thrombocytotic conditions in chronic hepatitis C brought about by the activated hepatic reticuloendothelial system, as caused by inflammation through the mechanism involving the activation of Kupffer cells.

The role of platelets in the pathogenesis of chronic hepatitis and cirrhosis is not clear. We suggest that platelet-derived factor and liver condition should be taken into account when examining the role of platelets in the liver. We identified a dense population of cells expressing PDGF receptor-β in the periportal areas of cirrhotic liver, whereas only a few mesenchymal cells stained for this peptide were seen in patients at the lower stage of chronic hepatitis and in controls. In addition, most of the PDGF receptor-β expressing cells were also stained for smooth muscle actin. These cells, which play a central role in liver fibrosis, are believed to be transformed from HSCs [29–31], and their proliferation is stimulated by PDGF [42]. HSCs are increasingly being seen as key mediators in the progression of liver fibrosis. In this study, HSCs expressing PDGF receptor-β were located in the periportal area, where platelets were frequently observed. PDGF is the basic mediator involved in platelet granules. PDGF overexpression has been linked to different types of fibrotic disorders and malignancies [43]. In chronic liver disease, the essential role of all PDGF family members in liver fibrosis has been demonstrated [42, 44–47]. To date, four members of the PDGF family have been identified: PDGF-A, PDGF-B, PDGF-C, and PDGF-D [48]. PDGF-B has a stimulating influence on the fibrogenesis and mitogenesis of HSCs in the liver [42]. The biological effects of PDGF are elicited through binding to two specific receptors, PDGF receptor-α and PDGF receptor-β. The binding affinity of PDGF receptor-β is restricted to PDGF-B [49]. When HSCs expressing PDGF receptor-β are present in the liver, the liver may be susceptible to PDGF contained in platelets. The accumulation of platelets in the liver with chronic hepatitis may be involved in liver fibrosis through the activated HSCs.

We also found that the platelet area was significantly smaller in cancerous tissue than that in noncancerous tissues. It has been reported that the number of Kupffer cells in cancerous tissues decreased in comparison with the number in noncancerous tissues as the histological differentiation of HCC decreased [50]. Indeed, the Kupffer cell area in cancerous tissues was significantly smaller than that in noncancerous tissues and tended to decrease with decreasing histological differentiation of HCC in this study. We consider that platelets may also accumulate in the blood space in cancerous tissue through some mechanisms involving the Kupffer cells.

In conclusion, the results obtained in the present study indicate that the accumulation of platelets in the liver with chronic hepatitis C may be involved in thrombocytopenia and liver fibrosis through the activated HSCs. In addition, platelets may accumulate in the sinusoidal space through another mechanism involving the activation of Kupffer cells. Further study of the biological characteristics and

function of these cells will contribute to improving the treatment of thrombocytopenia and liver fibrosis.

Conflict of interest The authors declare that they have no conflict of interest.

References

1. Mannaioni PF, Di Bello MG, Masini E. Platelets and inflammation: role of platelet-derived growth factor, adhesion molecules and histamine. Inflamm Res. 1997;46:4–18.
2. Handagama PJ, George JN, Shuman MA, McEver RP, Bainton DF. Incorporation of a circulating protein into megakaryocyte and platelet granules. Proc Natl Acad Sci USA. 1987;84:861–5.
3. Verheul HMW, Hoekman K, Bakker SL, Eekman CA, Folman CC, Broxterman HJ, et al. Platelet: transporter of vascular endothelial growth factor. Clin Cancer Res. 1997;3:2187–90.
4. Italiano JE Jr, Richardson JL, Patel-Hett S, Battinelli E, Zaslavsky A, Short S, et al. Angiogenesis is regulated by a novel mechanism: pro- and antiangiogenic proteins are organized into separate platelet α granules and differentially released. Blood. 2008;111:1227–33.
5. Brill A, Dashevsky O, Rivo J, Gozal Y, Varon D. Platelet-derived microparticles induce angiogenesis and stimulate post-ischemic revascularization. Cardiovasc Res. 2005;67:30–8.
6. Janowska-Wieczorek A, Wysoczynski M, Kijowski J, Marquez-Curtis L, Machalinski B, Ratajczak J, et al. Microvesicles derived from activated platelets induce metastasis and angiogenesis in lung cancer. Int J Cancer. 2005;113:752–60.
7. Gilsanz F, Escalante F, Auray C, Olbes AG. Treatment of leg ulcers in β-thalassaemia intermedia: use of platelet-derived wound healing factors from the patient's own platelets. Br J Haematol. 2001;115:710.
8. Mazzucco L, Medici D, Serra M, Panizza R, Rivara G, Orecchia S, et al. The use of autologous platelet gel to treat difficult-to-heal wounds: a pilot study. Transfusion. 2004;44:1013–8.
9. Lesurtel M, Graf R, Aleil B, Walther DJ, Tian Y, Jochum W, et al. Platelet-derived serotonin mediates liver regeneration. Science. 2006;312:104–7.
10. Nash GF, Turner LF, Scully MF, Kakkar AK. Platelets and cancer. Lancet Oncol. 2002;3:425–30.
11. Camerer E, Qazi AA, Duong DN, Cornelissen I, Advincula R, Coughlin SR. Platelets, protease-activated receptors, and fibrinogen in hematogenous metastasis. Blood. 2004;104:397–401.
12. Iannacone M, Sitia G, Isogawa M, Marchese P, Castro MG, Lowenstein PR, et al. Platelets mediate cytotoxic T lymphocyte-induced liver damage. Nat Med. 2005;11:1167–9.
13. Lang PA, Contaldo C, Georgiev P, El-Badry AM, Recher M, Kurrer M, et al. Aggravation of viral hepatitis by platelet-derived serotonin. Nat Med. 2008;14:756–61.
14. Bataller R, Brenner DA. Liver fibrosis. J Clin Invest. 2005; 115:209–18.
15. Friedman SL. Liver fibrosis-from bench to bedside. J Hepatol. 2003;38(Suppl 1):S38–53.
16. Witters P, Freson K, Verslype C, Peerlinck K, Hoylaerts M, Nevens F, et al. Review article: blood platelet number and function in chronic liver disease and cirrhosis. Aliment Pharmacol Ther. 2008;27:1017–29.
17. Aoki Y, Hirai K, Tanikawa K. Mechanism of thrombocytopenia in liver cirrhosis: kinetics of indium-111 tropolone labelled platelets. Eur J Nucl Med. 1993;20:123–9.
18. Schmidt KG, Rasmussen JW, Bekker C, Madsen PE. Kinetics and in vivo distribution of 111-In-labelled autologous platelets in chronic hepatic disease: mechanisms of thrombocytopenia. Scand J Haematol. 1985;34:39–46.
19. Toghill PJ, Green S. Splenic influences on the blood in chronic liver disease. Q J Med. 1979;48:613–25.
20. Aster RH. Pooling of platelets in the spleen: role in the pathogenesis of "hypersplenic" thrombocytopenia. J Clin Invest. 1966; 45:645–57.
21. Peck-Radosavljevic M. Thrombocytopenia in liver disease. Can J Gastroenterol. 2000;14:60D–6D.
22. Kajihara M, Okazaki Y, Kato S, Ishii H, Kawakami Y, Ikeda Y, et al. Evaluation of platelet kinetics in patients with liver cirrhosis: similarity to idiopathic thrombocytopenic purpura. J Gastroenterol Hepatol. 2007;22:112–8.
23. Noguchi H, Hirai K, Aoki Y, Sakata K, Tanikawa K. Changes in platelet kinetics after a partial splenic arterial embolization in cirrhotic patients with hypersplenism. Hepatology. 1995;22: 1682–8.
24. Kinuya K, Matano S, Nakashima H, Taki S. Scintigraphic prediction of therapeutic outcomes of splenectomy in patients with thrombocytopenia. Ann Nucl Med. 2003;17:161–4.
25. Sata M, Yano Y, Yoshiyama Y, Ide T, Kumashiro R, Suzuki H, et al. Mechanism of thrombocytopenia induced by interferon therapy for chronic hepatitis B. J Gastroenterol. 1997;32: 206–10.
26. Desmet VJ, Gerber M, Hoofnagle JH, Manns M, Scheuer PJ. Classification of chronic hepatitis: diagnosis, grading and staging. Hepatology. 1994;19:1513–20.
27. Batts KP, Ludwig J. Chronic hepatitis. An update on terminology and reporting. Am J Surg Pathol. 1995;19:1409–17.
28. Hirohashi S, Blum HE, Ishak KG, Deugnier Y, Kojiro M, Laurent Puig P, et al. Tumours of the liver and intrahepatic bile ducts. Hepatocellular carcinoma. In: Hamilton SR, Aaltonen LA, editors. Pathology and genetics of tumor of the digestive system. World Health Organization Classification of Tumors. Lyon: IARC Press; 2000. p. 159–72.
29. Pinzani M, Milani S, Herbst H, DeFranco R, Grappone C, Gentilini A, et al. Expression of platelet-derived growth factor and its receptors in normal human liver and during active hepatic fibrogenesis. Am J Pathol. 1996;148:785–800.
30. Blomhoff R, Wake K. Perisinusoidal stellate cells of the liver: important roles in retinol metabolism and fibrosis. FASEB J. 1991;5:271–7.
31. Ikura Y, Morimoto H, Ogami M, Jomura H, Ikeoka N, Sakurai M. Expression of platelet-derived growth factor and its receptor in livers of patients with chronic liver disease. J Gastroenterol. 1997;32:496–501.
32. Hill-Zobel RL, McCandless B, Kang SA, Chikkappa G, Tsan MF. Organ distribution and fate of human platelets: studies of asplenic and splenomegalic patients. Am J Hematol. 1986;23:231–8.
33. Furie B, Furie BC. Mechanisms of thrombus formation. N Engl J Med. 2008;359:938–49.
34. Bussolino F, Camussi G, Baglioni C. Synthesis and release of platelet-activating factor by human vascular endothelial cells treated with tumor necrosis factor or interleukin 1α. J Biol Chem. 1988;263:11856–61.
35. Miyazawa Y, Tsutsui H, Mizuhara H, Fujiwara H, Kaneda K. Involvement of intrasinusoidal hemostasis in the development of concanavalin A-induced hepatic injury in mice. Hepatology. 1998;27:497–506.
36. Rehermann B, Nascimbeni M. Immunology of hepatitis B virus and hepatitis C virus infection. Nat Rev Immunol. 2005;5: 215–29.
37. Spengler U, Nattermann J. Immunopathogenesis in hepatitis C virus cirrhosis. Clin Sci. 2007;112:141–55.
38. Dolganiuc A, Norkina O, Kodys K, Catalano D, Bakis G, Marshall C, et al. Viral and host factors induce macrophage activation and loss of toll-like receptor tolerance in chronic HCV infection. Gastroenterology. 2007;133:1627–36.

39. Pearson JM, Schultze AE, Jean PA, Roth RA. Platelet participation in liver injury from Gram-negative bacterial lipopolysaccharide in the rat. Shock. 1995;4:178–86.
40. Itoh H, Cicala C, Douglas GJ, Page CP. Platelet accumulation induced by bacterial endotoxin in rats. Thromb Res. 1996; 83:405–19.
41. Nakamura M, Shibazaki M, Nitta Y, Endo Y. Translocation of platelets into Disse spaces and their entry into hepatocytes in response to lipopolysaccharides, interleukin-1 and tumour necrosis factor: the role of Kupffer cells. J Hepatol. 1998;28: 991–9.
42. Pinzani M, Gesualdo L, Sabbah GM, Abboud HE. Effects of platelet-derived growth factor and other polypeptide mitogens on DNA synthesis and growth of cultured rat liver fat-storing cells. J Clin Invest. 1989;84:1786–93.
43. Dirks RP, Bloemers HP. Signals controlling the expression of PDGF. Mol Biol Rep. 1996;22:1–24.
44. Borkham-Kamphorst E, van Roeyen CRC, Ostendorf T, Floege J, Gressner AM, Weiskirchen R. Pro-fibrogenic potential of PDGF-D in liver fibrosis. J Hepatol. 2007;46:1064–74.
45. Czochra P, Klopcic B, Meyer E, Herkel J, Garcia-Lazaro JF, Thieringer F, et al. Liver fibrosis induced by hepatic overexpression of PDGF-B in transgenic mice. J Hepatol. 2006;45: 419–28.
46. Friedman SL. Mechanisms of hepatic fibrogenesis. Gastroenterology. 2008;134:1655–69.
47. Maass T, Thieringer FR, Mann A, Longerich T, Schirmacher P, Strand D, et al. Liver specific overexpression of platelet-derived growth factor-B accelerates liver cancer development in chemically induced liver carcinogenesis. Int J Cancer. 2011;128:1259–68.
48. Li X, Eriksson U. Novel PDGF family members: PDGF-C and PDGF-D. Cytokine Growth Factor Rev. 2003;14:91–8.
49. Kelly JD, Haldeman BA, Grant FJ, Murray MJ, Seifert RA, Bowen-Pope DF, et al. Platelet-derived growth factor (PDGF) stimulates PDGF receptor subunit dimerization and intersubunit trans-phosphorylation. J Biol Chem. 1991;266:8987–92.
50. Tanaka M, Nakashima O, Wada Y, Kage M, Kojiro M. Pathomorphological study of Kupffer cells in hepatocellular carcinoma and hyperplastic nodular lesions in the liver. Hepatology. 1996; 24:807–12.

Cancer Science
The official journal of the Japanese Cancer Association JCA

Interaction of endothelial progenitor cells expressing cytosine deaminase in tumor tissues and 5-fluorocytosine administration suppresses growth of 5-fluorouracil-sensitive liver cancer in mice

Takuji Torimura,[1,4,5] Takato Ueno,[1] Eitaro Taniguchi,[1] Hiroshi Masuda,[1] Hideki Iwamoto,[1] Toru Nakamura,[1] Kinya Inoue,[1] Osamu Hashimoto,[1] Mitsuhiko Abe,[1] Hironori Koga,[1] Vincenza Barresi,[2] Emi Nakashima,[3] Hirohisa Yano[4] and Michio Sata[1]

[1]Liver Cancer Division, Research Center for Innovative Cancer Therapy and Division of Gastroenterology, Department of Medicine, Kurume University School of Medicine, Kurume, Japan; [2]Department of Chemical Sciences, Section of Biochemistry and Molecular Biology, University of Catania, Catania, Italy; [3]Faculty of Pharmacy, Keio University, Tokyo; [4]Department of Pathology, Kurume University School of Medicine, Kurume, Japan

(Received September 5, 2011/Revised December 2, 2011/Accepted December 5, 2011/Accepted manuscript online December 8, 2011/Article first published online January 25, 2012)

The drug delivery system to tumors is a critical factor in upregulating the effect of anticancer drugs and reducing adverse events. Recent studies indicated selective migration of bone marrow-derived endothelial progenitor cells (EPC) into tumor tissues. Cytosine deaminase (CD) transforms nontoxic 5-fluorocytosine (5-FC) into the highly toxic 5-fluorouracil (5-FU). We investigated the antitumor effect of a new CD/5-FC system with CD cDNA transfected EPC for hepatocellular carcinoma (HCC) in mice. We used human hepatoma cell lines (HuH-7, HLF, HAK1-B, KYN-2, KIM-1) and a rat EPC cell line (TR-BME-2). *Escherichia coli* CD cDNA was transfected into TR-BME-2 (CD-TR-BME). The inhibitory effect of 5-FU on the proliferation of hepatoma cell lines and the inhibitory effect of 5-FU secreted by CD-TR-BME and 5-FC on the proliferation of co-cultured hepatoma cells were evaluated by a tetrazolium-based assay. In mouse subcutaneous xenograft models of KYN-2 and HuH-7, CD-TR-BME was transplanted intravenously followed by 5-FC injection intraperitoneally. HuH-7 cells were the most sensitive to 5-FU and KYN-2 cells were the most resistant. CD-TR-BME secreted 5-FU and inhibited HuH-7 proliferation in a 5-FC dose-dependent manner. CD-TR-BME were recruited into the tumor tissues and some were incorporated into tumor vessels. Tumor growth of HuH-7 was significantly suppressed during 5-FC administration. No bodyweight loss, ALT abnormality or bone marrow suppression was observed. These findings suggest that our new CD/5-FC system with CD cDNA transfected EPC could be an effective and safe treatment for suppression of 5-FU-sensitive HCC growth. (*Cancer Sci* 2012; 103: 542–548)

In 1997, putative endothelial progenitor cells (EPC) were isolated from peripheral blood and shown to be incorporated into the vasculature in adults.[1] The EPC in adults originate from the bone marrow and selectively home to sites with ongoing vascular formation.[2,3]

Vascular development is essential for the growth of solid tumors.[4,5] Accumulating evidence suggests that circulating bone marrow-derived cells, including EPC, migrate into tumor-associated stroma to support vascular formation and tumor development.[6,7] Stromal-derived factor-1 (SDF-1) mainly recruits bone marrow-derived cells to tumor tissues from the peripheral circulation.[8]

Cytosine deaminase (CD) in bacteria and fungi are known to deaminate 5-fluorocytosine (5-FC) to the highly toxic 5-fluorouracil (5-FU).[9,10] Normal mammalian cells do not have CD and are relatively resistant to 5-FC. Gene transfer of *Escherichia coli* CD to mammalian cells renders these cells selectively sensitive to the toxic effects of 5-FC. In many reports of cancer gene therapy with this suicide gene/prodrug system, the most interesting property is the "bystander effect", the death of unmodified tumor cells by 5-FU secretion from CD cDNA transfected cells.[11] Most of these reports have demonstrated the efficacy of the suicide gene/prodrug system.

Hepatocellular carcinoma (HCC) is one of the most common malignant tumors in the tropics and Far East, including Japan.[12] Hepatocellular carcinoma develops multifocally in the cirrhotic liver. Hepatocellular carcinoma is a highly angiogenic tumor, ultimately supplied with neoarteries in parallel with tumor development.[13,14] For advanced non-resectable HCC, chemotherapy with 5-FU is sometimes selected.[15,16] However, the therapeutic efficacy of 5-FU is not fully satisfactory due to liver dysfunction, leukocytopenia and thrombocytopenia caused by the associated liver cirrhosis. To improve the outcome of chemotherapy with 5-FU, it seems important to establish a new drug delivery system to supply a sufficient amount of 5-FU to HCC tissue only without severe adverse effects.

In the present study, we injected rat-derived endothelial progenitor cells, which were transfected with *E. coli* CD cDNA, and administered 5-FC to tumor-bearing mice to evaluate the antitumor effect of the new CD/5-FC system for HCC.

Materials and Methods

Reagents, cells and animals. HUVEC and human hepatoma cell lines (HuH-7, HLF) were obtained from CAMBREX Bio Science Walkersville Inc. (Walkersville, MD, USA). Human hepatoma cell lines (KYN-2, KIM-1, HAK1-B) were provided from the Department of Pathology, Kurume University School of Medicine (Kurume, Japan). TR-BME-2 cells, a cell line derived from rat bone marrow EPC were provided by the Department of Pharmaceutics, Keio University (Tokyo, Japan).[17] Male 5-week-old nude mice (BALB/c nu/nu, Kyudou KK, Fukuoka, Japan) were acclimatized and placed in separate cages. All animals received humane care according to the criteria outlined in the *Guide for the Care and Use of Laboratory Animals* prepared by the National Academy of Sciences and published by the National Institute of Health.[18] The experimental protocol was approved by the Laboratory Animal Care and Use Committee of Kurume University.

Plasmid construction and *in vitro* transfection. A retroviral vector, containing the entire coding sequence of the *E. coli* CD

[5]To whom correspondence should be addressed.
E-mail: tori@med.kurume-u.ac.jp

doi: 10.1111/j.1349-7006.2011.02182.x

gene (pLXSP-CD), was provided by D. F. Condorelli (Department of Chemical Science, Section of Biochemistry and Molecular Biology, University of Catania, Catania, Italy). Transfection of plasmid was performed according to the report by Barresi *et al.*[19]

***In vitro* inhibition of cell proliferation by addition of 5-FU.** Approximately 1000 HUVEC and TR-BME-2 cells transfected with CD cDNA (CD-TR-BME) were added with EGM-2 (Clonetics, San Diego, CA, USA) supplemented with 5% FBS to 96-well plates coated with human fibronectin (Gibco Invitrogen Co., Grand Island, NY, USA) and type 1 collagen (Gibco Invitrogen Co.). Then, 1×10^3 HuH-7, HLF, KIM-1, KYN-2 and HAK1-B in DMEM (Gibco Invitrogen Co.) supplemented with 10% FBS were added. HUVEC, CD-TR-BME cells and human hepatoma cells were incubated at 37°C. After 24 h, 5-FU at 0, 5, 10, 50, 100, 500 or 1000 ng/mL was added to the medium and incubated for 72 h. The cytotoxicity was then evaluated by a tetrazolium-based assay (Cell Count Reagent SF; Nakalai Tesque Inc., Kyoto, Japan).

5-Fluorouracil production by CD-TR-BME cells after the addition of 5-FC. Next, 5×10^4 CD-TR-BME cells were cultured with 1 mL of EBM-2 supplemented with 5% FBS for 24 h at 37°C. Then, 5-FC at 0, 1, 10, 100 or 1000 μg/mL was added to the medium and incubated for 72 h. The concentration of 5-FU in the media was measured using HPLC.

***In vitro* "bystander effect" experiment.** Next, 5×10^3 hepatoma cells (HuH-7, HuH-7, HLF, KIM-1, KYN-2, HAK1-B) were cultured with DMEM supplemented with 10% FBS for 24 h. After confirming that CD-TR-BME cells could not migrate through a 2-μm pore size filter of Chemotaxicell cell-culture chambers (Kurabo Inc., Osaka, Japan), CD-TR-BME cells (5×10^4) were cultured in the chambers with EBM-2 medium containing 5% FBS for 24 h at 37°C. The chambers with the CD-TR-BME cells were then co-cultured with hepatoma cells with EBM-2 medium containing 5% FBS and 5-FC for 72 h. The cytotoxicity against the hepatoma cells was evaluated by a tetrazolium-based assay.

Protocols of treatment with a combination of CD-TR-BME cells and 5-FC. Male nude mice were injected subcutaneously with 5×10^6 HuH-7 cells or KYN-2 cells. After the tumor volume reached 50 mm^3, the mice were divided at random into three groups: the PBS-treated group; the CD-TR-BME cell-injected group; and the CD-TR-BME cells treated with 5-FC group, respectively. After tumor formation, mice of the CD-TR-BME and CD-TR-BME + 5-FC groups received injections of 100 μL of PBS containing 1×10^6 CD-TR-BME cells via the tail vein for 5 days. Mice of the CD-TR-BME + 5-FC group received an intraperitoneal injection of 500 mg/kg of 5-FC for 10 days. All mice were then bred without any treatment for 7 days. Tumor size was measured by calipers in two dimensions every 3 days. The mice were killed at day 21. Tumor volume was calculated by the following equation: length × $width^2$ × 0.52.

Total RNA extraction and RT-PCR. For total RNA isolation, CD-TR-BME cells or 100 mg of tumor tissues were extracted with Isogen (Nippon Gene, Tokyo, Japan). cDNA was synthesized using 2 μg total RNA. The 20-μL RT reaction consisted of 5× first strand buffer, 0.5 mM dNTP, 50 nM random primers and 20 U SuperScript III reverse transcriptase (Invitrogen, Carlsbad, CA, USA). The RNA and primers were mixed and denatured by heating at 70°C for 10 min; the reverse transcription reaction mixture was then incubated for 30 min at 50°C, followed by 15 min at 70°C. The resulting cDNA was amplified by PCR with primer pairs specific for CD, SDF-1, CXCR4 and GAPDH (Table 1). The PCR products were resolved in 1.5% agarose gels and visualized by ethidium bromide staining and ultraviolet trans-illumination.

Migration of CD-TR-BME cells to tumor tissue and confocal laser scanning microscopy. The CD-TR-BME cells were labeled with PKH26-red (Sigma Chemical Co., St Louis, MO, USA).

Table 1. Primers used in RT-PCR

Gene	Annealing T (°C)	Primer sequences	PCR products (bp)
CD	54	5′-GGA GGCTAACAATGTCGAAT 3′-ATGTTTGCAACTTGCTGACC	1302
Murine SDF-1	60	5′-GGACGCCAAGGTCGTCGCCGTG 3′-TTGCATCTCCCACCCATGTCAG	335
Rat CXCR4	54	5′-ATGGGTTGGTAATCCTGGTC 3′-AGAGTAGGACCGGAAGTAGT	224
GAPDH	60	5′-ACCACAGTCCATGCCATCAC 3′-ATGTCGTTGTCCCACCACCT	452

CD, cytosine deaminase; SDF-1, stromal cell-derived factor-1.

Sections of tumor tissues were fixed with acetone and incubated overnight with rat anti-mouse CD 31 antibody (Research Diagnostics Inc., Flanders, NJ, USA) or rabbit anti-human SDF-1 antibody (Santa Cruz Biotechnology, Inc., Santa Cruz, CA, USA) at 4°C. The sections were then incubated with FITC-conjugated anti-rabbit IgG (DAKO Japan Inc., Kyoto, Japan) or FITC-conjugated anti-rat IgG (CHEMICON INTERNATIONAL, Temecula, CA, USA) for 30 min with TO-PRO-3 iodide (Invitrogen) for nuclei labeling at room temperature. Each incubation was followed by three washes with PBS. Four color imaging was performed (Z-series, 63× oil magnification, Zeiss LSM 510-Meta Confocal Microscope; Carl Zeiss Inc., Jena, Germany). Two independent hepatologists counted the number of CD31-positive vessels of tumor tissues obtained from mice treated with PBS at day 15 ($n = 6$), only CD-TR-BME cells at day 15 ($n = 6$) and CD-TR-BME cells plus 5-FC at day 8 ($n = 6$) and day 15 ($n = 6$). In each group, 30 random fields were selected blindly.

Tissue and serum 5-FU concentrations and serum α-fetoprotein (AFP) levels. At days 8 and 15 of the experiment, tumor tissues of HuH-7 cells and sera were collected from tumor-bearing mice injected with CD-TR-BME cells and treated with 5-FC ($n = 6$). Then, 1 g of wet tumor tissue was homogenized with 1 mL of PBS. The 5-FU concentrations in the tumor tissues and sera were measured on days 8 and 15 using HPLC. In addition, to measure the serum AFP levels, tumor-bearing mice treated with CD-TR-BME cells ($n = 6$) and mice injected with CD-TR-BME cells and treated with 5-FC ($n = 6$) were killed at day 15.

Alanine aminotransferase (ALT) levels, leukocytes, hemoglobin (Hb), platelet and bodyweight. Serum ALT activity was measured using a standard UV method. Bodyweight, peripheral leukocyte count, Hb level and platelet count were also measured. The above parameters were measured at day 15.

Statistical analysis. Data were expressed as mean ± SD. Differences between groups were examined for statistical significance using the Mann–Whitney *U*-test and the Kruskal–Wallis rank test. A *P*-value <0.05 denoted the presence of a statistically significant difference.

Results

5-Fluorouracil inhibits cell proliferation *in vitro*. 5-Fluorouracil inhibited the proliferation of HUVEC (IC_{50}, 100.4 ng/mL) and CD-TR-BME (IC_{50}, 99.8 ng/mL) in a dose-dependent manner. However, the proliferation of HUVEC and CD-TR-BME cells was not inhibited in the presence of up to 50 ng/mL of 5-FU concentration (Fig. 1A,B). In five hepatoma cell lines, HuH-7 (IC_{50}, 10.1 ng/mL) was the most sensitive to 5-FU, followed by HAK1-B (IC_{50}, 100 ng/mL), HLF (IC_{50}, 100.4 ng/mL), KIM-1 (IC_{50}, 449.7 ng/mL) and KYN-2 (IC_{50}, 449.8 ng/mL).

CD-TR-BME cells produce 5-FU after addition of 5-FC. CD-TR-BME cells secreted 5-FU into the media and the production level was 5-FC dose dependent (Fig. 1C). After 72 h, the final

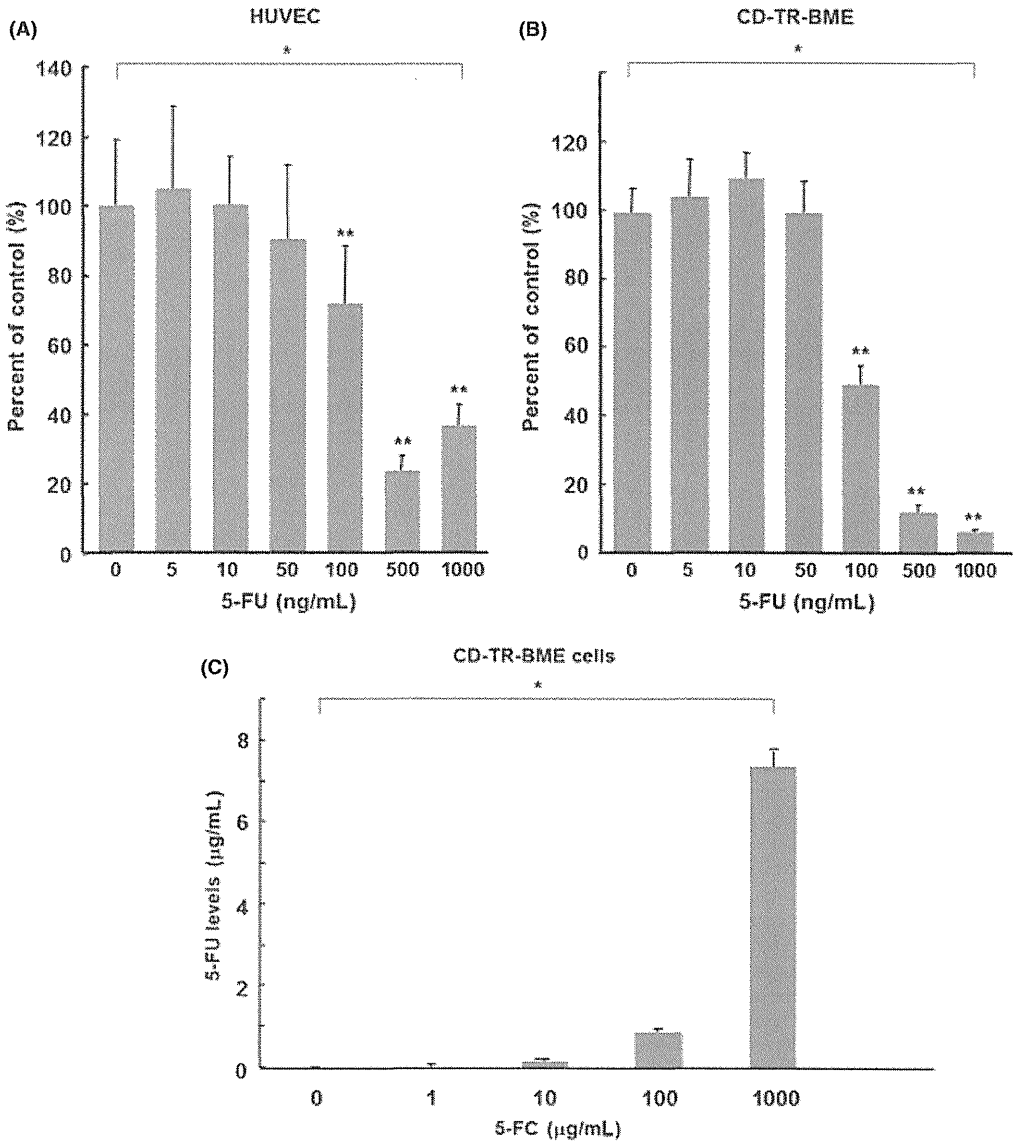

Fig. 1. Inhibition of cell proliferation by 5-fluorouracil (5-FU). (A) HUVEC, (B) CD-TR-BME. These cells were cultured with 10 mL of media containing 0–1000 ng/mL of 5-FU for 72 h. Cell proliferation was evaluated using a tetrazolium-based assay. Data are expressed relative to the control (n = 12). *P < 0.0001, using the Kruskal–Wallis test. **P < 0.0001, compared with the control group, using the Mann–Whitney U-test. (C) Secretion of 5-FU by CD-TR-BME cells with 5-fluorocytosine (5-FC). CD-TR-BME cells were cultured with 1 mL of the media containing 0–1000 mg/mL of 5-FC for 72 h. The concentration of 5-FU was measured. Data are expressed as mean ± SD of 12 samples. *P < 0.0001, using the Kruskal–Wallis test.

concentration of 5-FU secreted by the CD-TR-BME cells with 5-FC into the media was 7.4 ± 0.4 μg/mL.

"Bystander effect" of CD-TR-BME cells *in vitro*. After culture of the hepatoma cells with the chambers containing CD-TR-BME cells, the media significantly inhibited the proliferation of hepatoma cells in a 5-FC dose-dependent manner. HuH-7 was the most sensitive to 5-FC (IC_{50}, 0.89 μg/mL), followed by HAK1-B (IC_{50}, 10.3 μg/mL), KIM-1 (IC_{50}, 10.7 μg/mL), HLF (IC_{50}, 11.0 μg/mL) and KYN-2 (IC_{50}, 100.5 μg/mL) (Fig. 2). Proliferation of CD-TR-BME cells was suppressed in a 5-FC dose-dependent manner (data not shown). However, the proliferation of TR-BME cells was not suppressed with the addition of up to 1000 μg/mL 5-FC (data not shown).

Combination treatment with CD-TR-BME cells and 5-FC for a HuH-7 or KYN-2 cell xenograft model. HuH-7, the most sensitive to 5-FU, and KYN-2 cells, the most resistant, were used for *in vivo* experiments. In the HuH-7 cell xenograft model, at days 0, 3 and 6 of the initial treatment, there was no significant difference in tumor volume among the three groups. Since then, tumor volumes of the PBS-treated and CD-TR-BME groups continued to increase until day 21. From days 9 to 15, tumor growth in the CD-TR-BME + 5-FC mice was significantly suppressed compared with those of the other two groups. After completion of the 5-FC treatment, tumor volumes of CD-TR-BME + 5-FC mice started to increase rapidly and there was no significant difference in tumor volume of the three groups at day 21 (Fig. 3A,B). Serum AFP levels of the CD-TR-BME and CD-TR-BME + 5-FC mice at day 15 were 413 843 ± 203 129 and 113 436 ± 47 910 ng/mL, respectively. However, in the KYN-2 xenograft model, there was no significant difference in tumor volume among the three groups (Fig. 3C).

doi: 10.1111/j.1349-7006.2011.02182.x

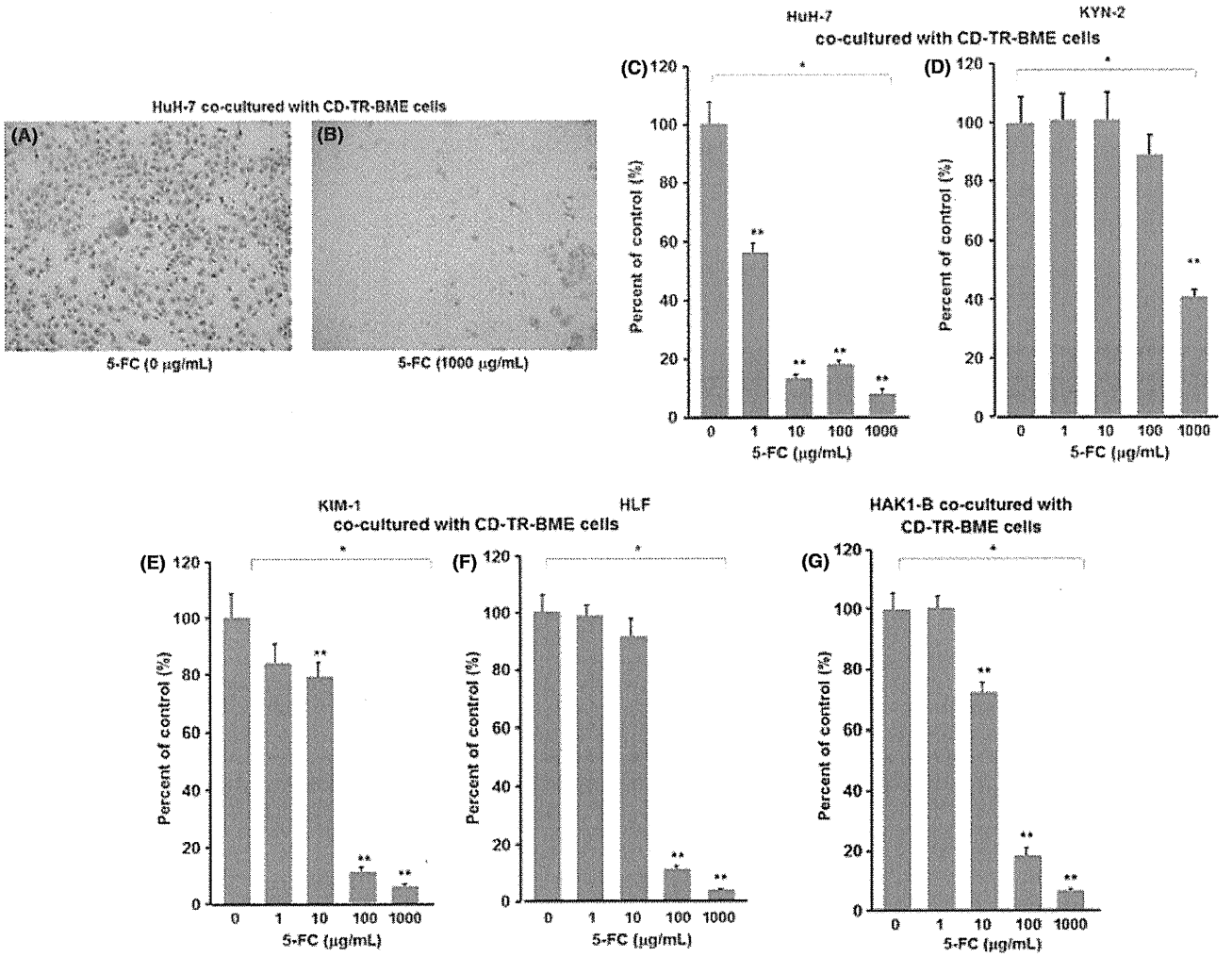

Fig. 2. Bystander effect of CD-TR-BME cells with 5-fluorocytosine (5-FC). Hepatoma cells were cultured in media containing 0–1000 mg/mL of 5-FC for 72 h with CD-TR-BME cells in chemotaxicell cell-culture chambers. (A) HuH-7 cells cultured with CD-TR-BME cells without 5-FC. (B) HuH-7 cells cultured with CD-TR-BME cells with 1000 mg/mL of 5-FC. (C–G) Cell proliferation was evaluated using a tetrazolium-based assay. Data are expressed relative to the control ($n = 12$) (C, HuH-7; D, KYN-2; E, KIM-1; F, HLF; G, HAK1-B). *$P < 0.0001$, using the Kruskal–Wallis test. **$P < 0.0001$, compared with the control group, using the Mann–Whitney U-test.

Migration of CD-TR-BME cells to tumor tissues and vascular density in tumor tissues. RT-PCR analysis showed SDF-1 expression in tumor tissues of HuH-7 cells and CXCR4 expression in the CD-TR-BME cells (Fig. 4A,B). Immunohistochemical analysis showed recruitment of the injected CD-TR-BME cells close to the SDF-1-expressing hepatoma cells (Fig. 4C). Examination at a higher magnification showed the incorporation of some CD-TR-BME cells into new blood vessels within the tumor tissues (Fig. 4D). However, most of these cells were localized in the interstitial tissues around the vessels in the tumor tissues (Fig. 4E). At 200-fold magnification, the numbers of CD31-positive vessels in tumor tissues of mice treated with PBS on day 15, CD-TR-BME cells on day 15 and CD-TR-BME cells plus 5-FC on days 8 and 15 were 7.2 ± 2.1, 7.2 ± 2.1, 6.9 ± 0.9 and 7.1 ± 2.1, respectively. There was no significant difference in vessel density among the groups.

5-Fluorouracil concentration in tumor tissues and sera. The 5-FU concentrations in the tumor tissues of HuH-7 cells at days 8 and 15 were 25.2 ± 14.2 and 22.4 ± 12.4 ng/mL, respectively. In all but one sample, serum 5-FU levels were not detected at days 8 and 15. Serum 5-FU concentrations of samples with detectable levels at days 8 and 15 were 8.4 and 7.3 ng/mL, respectively. These cases showed the highest tissue 5-FU concentrations at days 8 and 15, respectively.

Effect of CD-TR-BME and 5-FC treatment on leukocyte count, Hb, platelet count, serum ALT and bodyweight. Leukocyte count, Hb level and platelet count of CD-TR-BME-injected mice and CD-TR-BME + 5-FC-treated mice were 1600 ± 352/μL, 13.2 ± 1.9 g/dL, 46.3 ± 21.7 × 10^4/μL and 1800 ± 593/μL, 13.9 ± 1.2 g/dL, 48.8 ± 22.9 × 10^4/μL, respectively. Serum ALT levels of CD-TR-BME-injected mice and CD-TR-BME + 5-FC-treated mice were 38.5 ± 8.9 and 41.2 ± 7.8 U/L, respectively. The bodyweights of CD-TR-BME-injected mice and CD-TR-BME + 5-FC-treated mice were 25.2 ± 2.4 and 26.2 ± 2.9 g, respectively. There were no significant differences in leukocyte count, Hb level, platelet count, serum ALT level and bodyweight between CD-TR-BME-injected mice and CD-TR-BME + 5-FC-treated mice.

Discussion

In the *in vitro* study, HuH-7 cells were the most sensitive to 5-FU among five tested hepatoma cell lines. Furthermore, HuH-7 was more sensitive to 5-FU than CD-TR-BME cells and

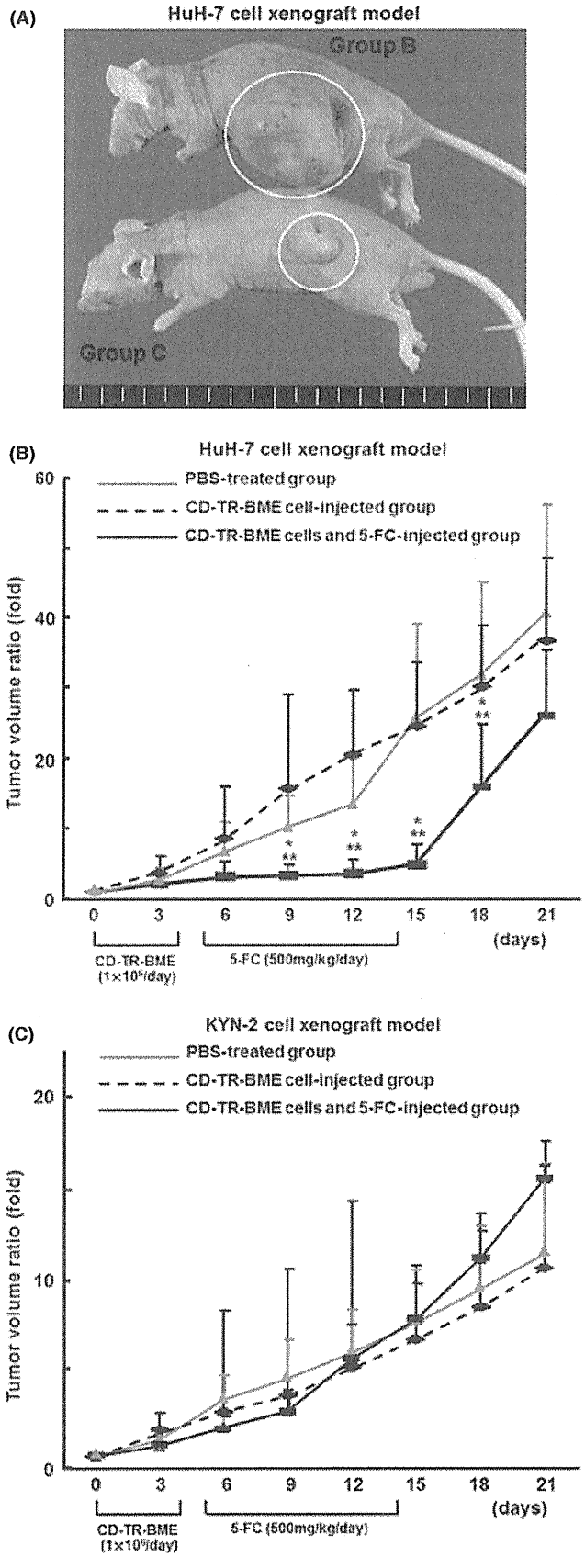

Fig. 3. Treatment of subcutaneous tumor with a combination of CD-TR-BME cells and 5-fluorocytosine (5-FC). (A) Tumors of HuH-7 cells at day 21. Group B, CD-TR-BME cells; Group C, CD-TR-BME cells + 5-FC. (B) Time-course observation of tumor volumes (HuH-7). Data are expressed relative to the control (day 0) ($n = 6$). $^{*}P < 0.05$, compared with the CD-TR-BME cell-injected group, using the Mann–Whitney U-test. $^{**}P < 0.05$, compared with PBS-treated cells, using the Mann–Whitney U-test. (C) Time-course observation of tumor volumes in the dorsal portion of mice (KYN-2). Data are expressed relative to the control (day 0) ($n = 6$).

HUVEC. The CD-TR-BME cells produced 5-FU into the media in a 5-FC dose-dependent manner. 5-Fluorocytosine and 5-FU are small and highly water-soluble molecules; they penetrate well into most body sites and do not require cell–cell contact for intercellular transfer.[20] CD-TR-BME cells seem to incorporate 5-FC into the cytoplasm, then produce and secrete 5-FU into the media without cell damage at relatively low concentrations of 5-FC. At higher concentrations of 5-FC, high concentrations of 5-FU in CD-TR-BME cells induce their apoptosis.

In the process of EPC homing from the bone marrow into the tumor microenvironment, vascular endothelial growth factor (VEGF) and SDF-1 undoubtedly play critical roles through specific interactions with CXCR4 and VEGFR-1 and VEGFR-2, respectively.[8,21] Recent data show that among these cytokines, VEGF mainly induces mobilization of EPC from the bone marrow into the circulation while SDF-1 recruits EPC to the tumor tissues.[22–31] In the present study, tumor tissues expressed SDF-1 and CD-TR-BME cells expressed CXCR4. Injected CD-TR-BME cells migrated to tumor tissues. Of course, there seems to be a possibility that some of the injected CD-TR-BME cells have migrated to other tissues such as non-cancerous liver tissue and bone marrow. Tamura *et al.*[23] reported that intravenously injected TR-BME cells were homed to tumor tissue with significantly higher specificity. Injected CD-TR-BME cells seemed to migrate mainly to tumor tissues through SDF-1 and CXCR4 interaction.

Interestingly, some of the injected CD-TR-BME cells were incorporated into vascular formation and others were distributed in the interstitial space of tumor tissue. Furthermore, intravenous injection of CD-TR-BME cells did not increase the vascular density in tumor tissues. These distribution patterns were also observed in tumor tissues with the injection of wild type EPC in our preliminary study. Another group reported that only some of the systemically injected EPC were incorporated into tumor vessels.[8] A wide range of cell types including endothelial cells were shown to transdifferentiate into tumor-associated-fibroblasts (TAF).[24] Residual CD-TR-BME cells might migrate to the interstitial space due to the enhanced permeability of tumor vessels and transdifferentiate into TAF.[25] In general, tumor tissues produce VEGF and SDF-1 to recruit an appropriate number of bone marrow-derived EPC for vasculogenesis.[2,4] We might have injected too many CD-TR-BME cells than what was required for vasculogenesis.

The concentrations of 5-FU in tumor tissues on days 8 and 15 of the treatment were 25.4 ± 13.0 and 22.4 ± 12.4 ng/g wet tissue, respectively. Serum 5-FU was not detected in any of the samples except for one on days 8 and 15, respectively. As the CD-TR-BME cells and EPC selectively migrate to tumor tissues, we assume that 5-FU was selectively produced by the CD-TR-BME cells in tumor tissues. Therefore, no adverse effects were observed. Treatment with 5-FC after CD-TR-BME cell injection did not reduce the vascular density in tumor tissues. In the *in vitro* study, proliferation of HUVEC and CD-TR-BME cells was not suppressed in the presence of up to 50 ng/mL of 5-FU, while proliferation of HuH-7 cells was suppressed by 36 and 52% at 10 and 50 ng/mL of 5-FU, respectively. The CD/5-FC system mainly suppressed tumor growth of HuH-7 cells in

doi: 10.1111/j.1349-7006.2011.02182.x

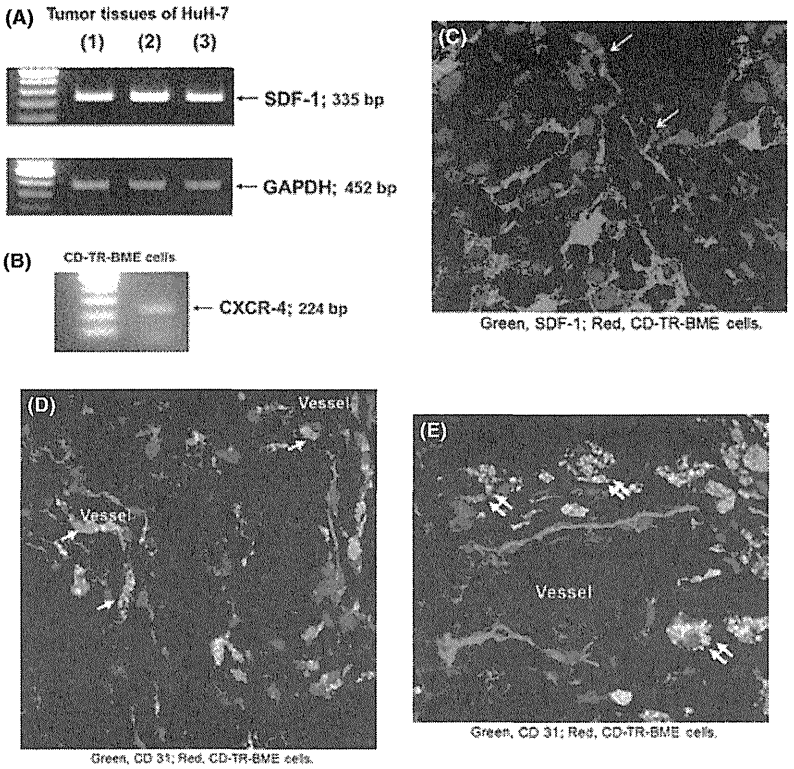

Fig. 4. Migration of CD-TR-BME cells to tumor tissues. (A) Expression of stromal-derived factor-1 (SDF-1) transcripts in tumor tissues (RT-PCR). Lanes 1–3, representative tumor tissues of HuH-7 cells. (B) Expression of CXCR4 transcripts in CD-TR-BME cells (RT-PCR). (C–E) Immunostaining of SDF-1 (green) and CD31 (green) with nuclear staining (blue) in tumor tissues of mice injected with CD-TR-BME cells labeled with red fluorescent marker PKH26-red. CD-TR-BME cells (red) (arrows) were recruited to tumor tissue close to SDF-1-expressing hepatoma cells (green) (C). CD-TR-BME cells (red) were incorporated into vessel walls (arrows) (D) or distributed within stromal tissue near a blood vessel (double arrows) (E).

the xenograft model by inhibiting tumor cell proliferation rather than an anti-angiogenic effect. However, The CD/5-FC system seems to be unable to maintain enough concentration of 5-FU to suppress the tumor growth of KYN-2 cells, which are 5-FU resistant. In the *in vitro* study, HuH-7 cells were more sensitive to 5-FU than KYN-2 cells. Since cell proliferation of KYN-2 cells was not suppressed in the presence of up to 100 ng/mL of 5-FU, the 5-FU concentration in tumor tissues seemed too low to suppress the tumor growth of KYN-2 cells *in vivo*. Miller *et al.*[26] reported that inherent 5-FU sensitivity is an important factor in determining efficacy of the CD/5-FC system. These findings indicate that diffusible 5-FU from CD-TR-BME cells in tumor tissues is at an optimal concentration to suppress the proliferation of HuH-7 cells. Furthermore, as the concentration of 5-FU in tumor tissues on day 15 of the treatment was maintained similar to that on day 8, the number of injected CD-TR-BME cells in tumor tissues did not seem to be decreased by the 5-FU produced by these cells.

Our CD/5-FC system with carrier cells enabled gene delivery to tumor tissues and repeated treatment by the escape from anti-vector immunity. However, for clinical application, the following issues must be resolved. First, the injected cells must be improved for more selective migration to tumor tissues. To improve selective migration to tumor tissues, gene transfection of CXCR4 or VEGF receptor (VEGFR) to CD-TR-BME cells might be necessary. Second, production of 5-FU in tumor tissues must be upregulated. To upregulate 5-FU production in tumor tissues, it might be necessary to increase the number of injected CD-TR-BME cells or to transfect more CD cDNA to TR-BME cells. However, high concentrations of 5-FU in tumor tissues induced apoptosis of CD-TR-BME cells as well as tumor cells. Repeated injections of CD-TR-BME cells will be required. The other possible way is to use a replication-competent oncolytic virus as the vector.[27,28] The replication-competent virus vector will be able to transfect CD cDNA to tumor cells and other kinds of cells in tumor tissues and upregulate 5-FU production. Third, tumor cell proliferation by injected CD-TR-BME cells must be inhibited. There were no significant differences in tumor volume and vascular density between the non-treated tumor group and the CD-TR-BME cell-injected tumor group. Furthermore, Sasajima *et al.*[29] reported that injection of vascular proangiogenic cells caused vascular remodeling and delay of tumor growth as well as a reduction of factors involved in drug resistance. As EPC produce VEGF, EGF, TGF-α and HGF,[30,31] these growth factors might stimulate tumor cell proliferation and angiogenesis.

In conclusion, we have demonstrated that injected CD cDNA-transfected endothelial progenitor cell lineage migrated to the tumor tissues of hepatoma cells and suppressed tumor growth by producing 5-FU in tumor tissues with intraperitoneal 5-FC injection. Our CD/5-FC system did not cause any severe adverse effects, suggesting that selective 5-FU production in tumor tissues with the character of EPC to home to tumor tissues might be a suitable strategy in the treatment of human HCC.

Acknowledgment

The authors thank Professor D. F. Condorelli for his kind supply of the *E. coli* CD gene (pLXSP-CD).

Disclosure Statement

The authors have no commercial affiliations and no financial relationships to disclose.

References

1 Asahara T, Murohara T, Isner JM *et al.* Isolation of putative progenitor endothelial cells for angiogenesis. *Science* 1997; **275**: 964–7.
2 Isner JM, Kalka C, Kawamoto A, Asahara T. Bone marrow as a source of endothelial cells for natural and iatrogenic vascular repair. *Ann NY Acad Sci* 2001; **953**: 75–84.
3 Vajkoczy P, Blum S, Hatzopoulos AK *et al.* Multistep nature of microvascular recruitment of *ex vivo*-expanded embryonic endothelial progenitor cells during tumor angiogenesis. *J Exp Med* 2003; **197**: 755–65.
4 Dome B, Hendrix MJ, Paku S, Tovari J, Timar J. Alternative vascularization mechanisms in cancer: pathology and therapeutic implications. *Am J Pathol* 2007; **170**: 1–15.
5 Folkman J. Tumor angiogenesis in women with node-positive breast cancer. *Cancer J Sci Am* 1995; **1**: 106–8.
6 Jin H, Aiyer A, Varner J *et al.* A homing mechanism for bone marrow-derived progenitor cell recruitment to the neovasculature. *J Clin Invest* 2006; **116**: 652–62.
7 Bagley RG, Weber W, Rouleau C, Teicher BA. Pericytes and endothelial precursor cells: cellular interactions and contributions to malignancy. *Cancer Res* 2005; **65**: 9741–50.
8 Orimo A, Gupta PB, Weinberg RA *et al.* Stromal fibroblasts present in invasive human breast carcinomas promote tumor growth and angiogenesis through elevated SDF-1/CXCL12 secretion. *Cell* 2005; **121**: 335–48.
9 Polak A, Scholer HJ. Mode of action of 5-fluorocytosine and mechanisms of resistance. *Chemotherapy* 1975; **21**: 113–30.
10 Dong Y, Wen P, Fine HA *et al.* *In vivo* replication-deficient adenovirus vector-mediated transduction of the cytosine deaminase gene sensitizes glioma cells to 5-fluorocytosine. *Hum Gene Ther* 1996; **7**: 713–20.
11 Kuriyama S, Kikukawa M, Tsujii T *et al.* Cytosine deaminase/5-fluorocytosine gene therapy can induce efficient anti-tumor effects and protective immunity in immunocompetent mice but not in athymic nude mice. *Int J Cancer* 1999; **81**: 592–7.
12 Di Bisceglie AM, Rustgi VK, Hoofnagle JH, Dusheiko GM, Lotze MT. NIH conference. Hepatocellular carcinoma. *Ann Intern Med* 1988; **108**: 390–401.
13 Matsui O, Kadoya M, Ida M *et al.* Benign and malignant nodules in cirrhotic livers: distinction based on blood supply. *Radiology* 1991; **178**: 493–7.
14 Honda H, Tajima T, Masuda K *et al.* Vascular changes in hepatocellular carcinoma: correlation of radiologic and pathologic findings. *AJR* 1999; **173**: 1213–7.
15 Ando E, Tanaka M, Sata M *et al.* Hepatic arterial infusion chemotherapy for advanced hepatocellular carcinoma with portal vein tumor thrombosis: analysis of 48 cases. *Cancer* 2002; **95**: 588–95.
16 Han KH, Seong J, Kim JK, Ahn SH, Lee DY, Chon CY. Pilot clinical trial of localized concurrent chemoradiation therapy for locally advanced hepatocellular carcinoma with portal vein thrombosis. *Cancer* 2008; **113**: 995–1003.
17 Hattori K, Muta M, Nakashima E *et al.* Establishment of bone marrow-derived endothelial cell lines from ts-SV40 T-antigen gene transgenic rats. *Pharm Res* 2001; **18**: 9–15.
18 Garber JC, Barbee RW. *Guide for the care and use of laboratory animals.* 1996 edn. Washington DC: The National Academies Press, 2000, 1–220.
19 Barresi V, Belluardo N, Sipione S, Mudo G, Cattanes E, Condorelli DF. Transplantation of prodrug-converting neural progenitor cells for brain tumor therapy. *Cancer Gene Ther* 2003; **10**: 396–402.
20 Haberkorn U, Oberdorfer F, Schackert HK *et al.* Monitoring gene therapy with cytosine deaminase: *in vitro* studies using tritiated-5-fluorocytosine. *J Nucl Med* 1996; **37**: 87–94.
21 Li B, Sharpe EE, Young PP *et al.* VEGF and PlGF promote adult vasculogenesis by enhancing EPC recruitment and vessel formation at the site of tumor neovascularization. *FASEB J* 2006; **20**: 1495–7.
22 Aghi M, Cohen KS, Klein RJ, Scadden DT, Chiocca EA. Tumor stromal-derived factor-1 recruits vascular progenitors to mitotic neovasculature, where microenvironment influences their differentiated phenotypes. *Cancer Res* 2006; **66**: 9054–64.
23 Tamura M, Unno K, Oku N *et al.* *In vivo* trafficking of endothelial progenitor cells their possible involvement in the tumor neovascularization. *Life Sci* 2004; **75**: 575–84.
24 Xouri G, Christian S. Origin and function of tumor stroma fibroblasts. *Semin Cell Dev Biol* 2010; **21**: 40–6.
25 Matsumura Y, Kataoka K. Preclinical and clinical studies of anticancer agent-incorporating polymer micelles. *Cancer Sci* 2009; **100**: 572–9.
26 Miller CR, Williams CR, Buchsbaum DJ, Gillespie GY. Intratumoral 5-fluorouracil produced by cytosine deaminase/5-fluorocytosine gene therapy is effective for experimental human glioblastomas. *Cancer Res* 2002; **62**: 773–80.
27 Power AT, Bell JC. Cell-based delivery of oncolytic viruses: a new strategic alliance for a biological strike against cancer. *Mol Ther* 2007; **15**: 660–5.
28 Willmon C, Harrington K, Kottke T, Prestwich R, Melcher A, Vile R. Cell carriers for oncolytic viruses: Fed Ex for cancer therapy. *Mol Ther* 2009; **17**: 1667–76.
29 Sasajima J, Mizukami Y, Kohgo Y *et al.* Transplanting normal vascular proangiogenic cells to tumor-bearing mice triggers vascular remodeling and reduces hypoxia in tumors. *Cancer Res* 2010; **70**: 6283–92.
30 Taniguchi E, Kin M, Torimura T *et al.* Endothelial progenitor cell transplantation improves the survival following liver injury in mice. *Gastroenterology* 2006; **130**: 521–31.
31 Nakamura T, Torimura T, Sata M *et al.* Significance and therapeutic potential of endothelial progenitor cell transplantation in a cirrhotic liver rat model. *Gastroenterology* 2007; **133**: 91–107.

doi: 10.1111/j.1349-7006.2011.02182.x